MiR-34a regulates Migration of Mouse Lung Fibroblasts by modulating PDGFR signalling

Inaugural Dissertation for acquirement of the Dr. med. Degree of the Faculty of Medicine of the Justus Liebig University Giessen

by

Philipp Friedrich David Arndt

of Hannover, Germany

Gießen, 2019

From the Institute of Max Planck Institute for Heart and Lung Research

Director/ Chairman: Prof. Dr. Werner Seeger

of the Faculty of Medicine of the Justus Liebig University Giessen

Supervisor: Prof. Dr. Werner Seeger

Committee Member: Prof. Dr. Saverio Bellusci

Date of Doctorial Defence: 21.10.2020

Table of contents

1 Introduction

Bronchopulmonary dysplasia (BPD) is a chronic respiratory disease following neonatal lung injury and is one of the most frequent complications following preterm delivery [1]. Pathologically BPD is marked by alveolar hypoplasia (**Fig. 1)** and abnormal vascular organization, impairing effective gas exchange, and consequently decreasing lung function through childhood and into adult life [2]. Different forms of therapy, for example antenatal steroids and surfactant replacement therapy, have been successfully developed to improve the outcome of BPD, but none so far have been known to cure or prevent the disease altogether [1, 3]. Also, the incidence of BPD has risen over the years due to increased survival of very low birth weight (VLBW) infants, due to recent improvements in modern medicine [4]. Therefore, it crucial to find new targets for treatment to improve the quality of life of those affected by the disease. The causes of BPD are manifold; one of them is the oxygen therapy to treat respiratory distress syndrome (RDS) after preterm birth. With that knowledge, research has identified molecules that seem to be altered by hyperoxia, one of them being microRNA (miR)-34a [5]. Knowing about the properties and potential of miR-34a as a future therapy option, miR-34a had become an interesting target. But the effect of miR-34a on migration in fibroblasts, a vital feature in lung development, specifically in relation to platelet-derived growth factor receptor (PDGFR), is yet to be investigated. The aim of this thesis is to investigate whether miR-34a has an effect on migration in fibroblast and what role PDGFR plays in this process, in order to reveal new knowledge that could lead to an alternative approach for BPD treatment.

1.1 Human lung development

The lung is the organ in which gaseous exchange takes place, which is essential for human survival. It is in the alveolar units of the lung where oxygen crosses into the bloodstream and in return, carbon dioxide exits the bloodstream and is therefore eliminated from the organism [6]. The lung consists of a highly complex tubular system, which is organized to form maximum surface area for extremely efficient gaseous exchange at the blood-air barrier [7, 8]. Human lung development can be divided into three developmental stages: The early embryonic period, the foetal period proper and the postnatal period. The foetal period can be further subdivided into three more phases: The pseudoglandular, the

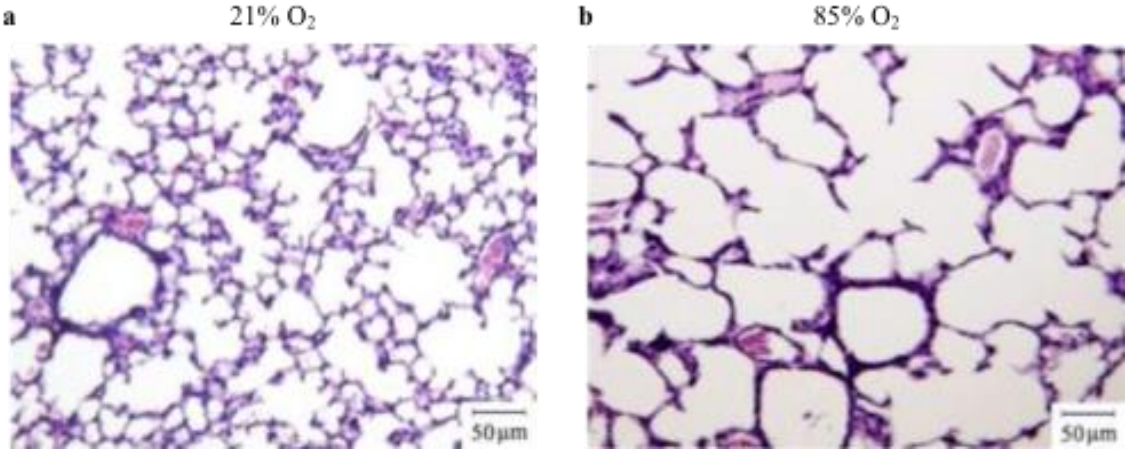

Figure 1. Alveolar hypoplasia in mice caused by hyperoxia exposure. A) Normal alveolarization after exposure to normoxia B) Alveolar hypoplasia and aberrant lung development due to hyperoxia exposure. Image adapted from [2].

canalicular and the saccular stage (**Fig. 2**). During the first seven weeks, the early embryonic period takes place, in which towards the end of week four, a primary lung bud appears from the ventral wall of the prospective oesophagus. This area expresses *Nkx2-1* [8]. Therefore, the epithelial constituents are derived from the endoderm, and the surrounding connective tissue from the mesoderm. As the bud rapidly grows into the surrounding mesenchyme by successive dichotomous division, the bud sets the basic framework for the conductive airways in the adult lung. At the same time, the pulmonary arteries develop from the sixth pair of aortic arches to form a vascular plexus around the lung tubules. At the end of the embryonic phase, the primitive lung resembles in shape a tubulo-acinar gland, hence the name of the following stage, the pseudoglandular stage. The pseudoglandular stage takes place during the weeks 7-17 in utero, which is marked by development of the prospective conductive airways and the arrival of the acinar outlines, through further branching at the periphery of the epithelial tubules. It is known that epithelial-mesenchymal interactions are crucial to the branching and differentiation of the epithelium [9]. The pseudoglandular stage is followed by the canalicular stage, it occurs in weeks 17 to 26. This stage is given its name by its newly formed airways called canaliculi, which are formed by more peripheral branching, lengthening and widening of the distal airspaces. Simultaneously, an increase in capillarization can be observed, forming the first air-blood barriers. The last stage before the postnatal period is the saccular stage, from week 24 to birth. In this stage, the last generation of airways are formed, the alveolar sacs. Because of the vast expansion of the airways, interstitial tissue

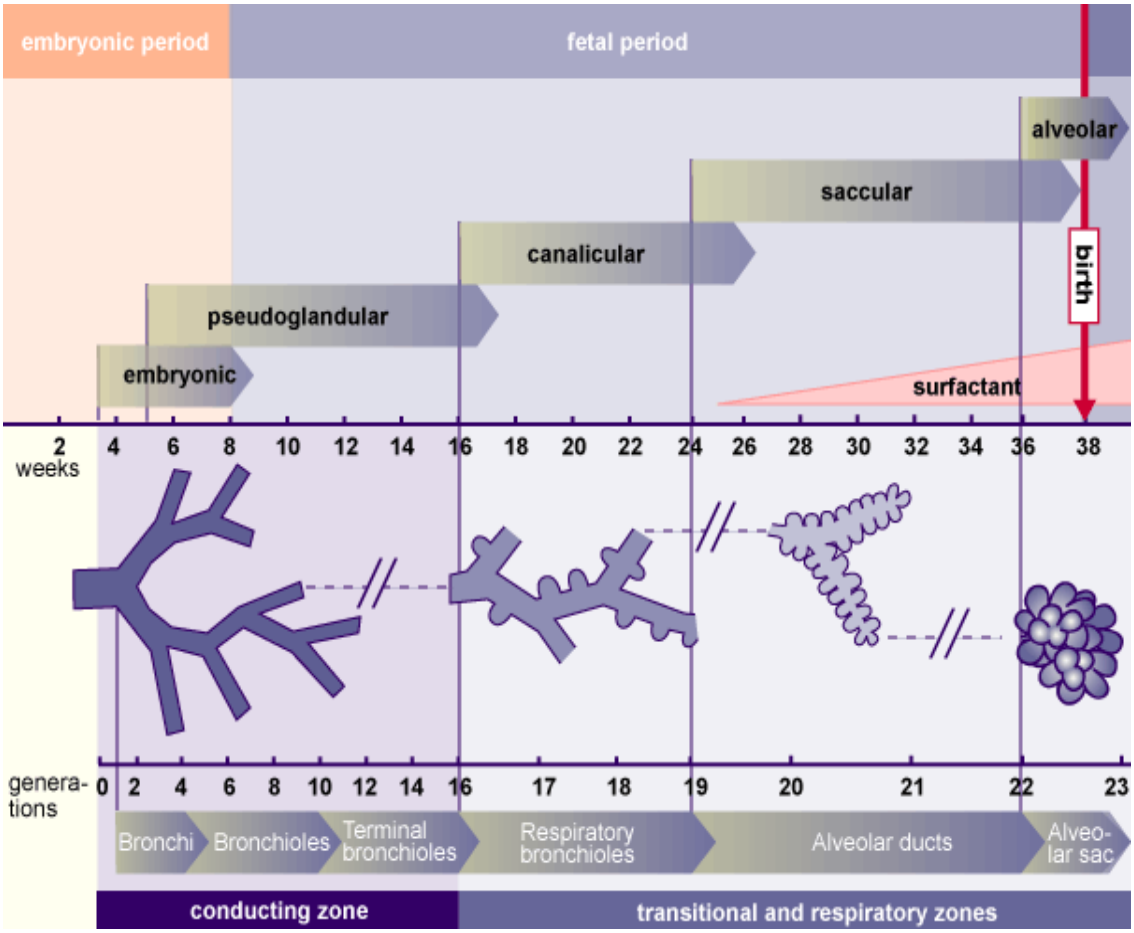

Figure 2. The stages of human lung development. Following the embryonic period, the fetal period takes place, which is further divided into pseudoglandular, canalicular, saccular and alveolar stages, which partially takes place postnatal. Image from [10]

becomes more and more scarce, eventually leaving only a capillary bilayer in the intersaccular septa. However, at birth, the lung is not fully developed, the lung has yet to form secondary septa, which subdivide the saccules to form alveoli. The further reduction of interstitial tissue causes alveoli and capillaries to appose closely and the capillary bilayer to merge into one layer, thus completing lung development. This process, which can take up to 8 years after birth, is called the postnatal period [7].

In conclusion, even though each developmental stage is essential to proper lung development, the most critical development occurs during late lung development.

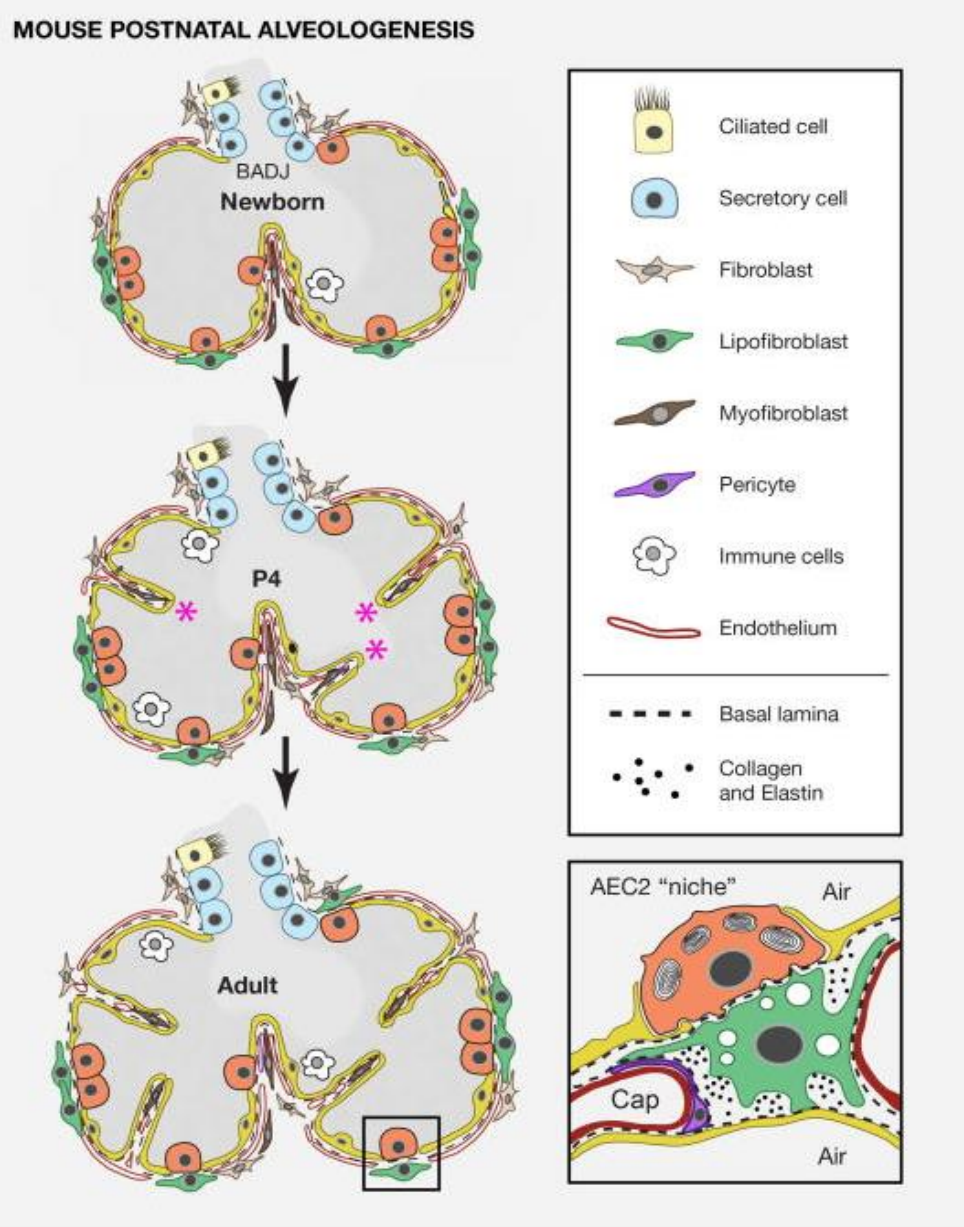

Figure 3. Late lung development in mice. Process of alveolarization by forming secondary septa. The newborn mouse only has primary septa, however at P4, secondary septa arise from crests of tissue (asterisks) containing blood vessels and stromal cells that migrate from the walls into the crests and differentiate into fibroblasts, which is the main producer of extra cellular matrix (ECM). In the adult lung, alveolarization is completed. BADJ: bronchoalveolar duct junction, Cap: Capillary, AEC: alveolar epithelial cell. Image adapted from [11].

1.2 Fibroblasts in late lung development of the mouse

While the stages of lung development are similar in human and mouse, the main difference is the length of gestation and consequently the timing of the developmental stages. For instance, lung development in mice starts as early as embryonic day (E) 8 and comes to an end at post-natal day (P) 21.5, whereas human lung development begins in week 4, and ends only years after birth [7, 12, 13].

The most crucial occurrence during late lung development is alveolarization by forming secondary septa, in which fibroblasts play an important role. At around P4, the secondary septa appear from an elevation on the wall of the alveolar sacs (**Fig. 3**). Then, stromal cells migrate into the secondary septa, to differentiate into pericytes, myofibroblasts, lipofibroblasts and other poorly characterized cell types [14]. The myofibroblasts are found at the extremity of the secondary septa and deposit elastin at the tip and at the shaft of the septa, creating a structure of flexible extracellular matrix that is crucial for breathing mechanics [15]. The lipofibroblasts, however, are closely associated with alveolar epithelial cells Type II (AEC2) and are said to support the AEC2 with surfactant production [11].

Therefore, the secondary septa further subdivide the alveolar sacs into smaller alveoli to maximize the surface area for gas exchange, thus concluding the postnatal developmental stage.

1.3 Bronchopulmonary dysplasia

Bronchopulmonary dysplasia is a chronic lung disease, that occurs as a result of neonatal lung injury, such as blunted secondary septation and mechanical ventilation with high oxygen percentage [16]. First described in 1967 by Northway and Colleagues, BPD has been redefined in 2000 by the National Institute of Child Health and Human Development (NICHD), for the first time taking different severities of the disease into account. Mild BPD was defined as the need for supplemental oxygen for ≥28 days, but not at 36-week postmenstrual age (PMA). Moderate BPD was determined as the need for supplemental oxygen for 28 days and at 36-week PMA at ≤30% O_2. Finally, Severe BPD was characterized as the need for supplementary oxygen for 28 days and at 36-week PMA at >30% O_2 and/or the need for mechanical ventilation [17, 18].

1.3.1 Causes of bronchopulmonary dysplasia

Causes for BPD are believed to be multiple, and they can be divided into internal, external and iatrogenic factors [1]. Beginning with internal factors, prematurity, so being born before week 37 of gestation seems to be the determining cause for BPD [19]. Especially being born during the saccular stage, occurring during weeks 23 to 32 of gestation, where the lung has yet to develop airway-supporting mechanisms, such as surfactant and antioxidant mechanisms, is a high risk for developing BPD. Other than prematurity, male gender [20] and genetic predisposition [21] are thought to be internal factors to promote BPD. Postnatal infection, as an external factor has also been found to increase the risk of BPD [22]. Iatrogenic factors include oxygen treatment and mechanical ventilation, measures taken in order to treat respiratory distress syndrome (RDS) caused by preterm birth. Although it is unknown how much oxygen exactly is harmful to the lung, it has been reported that infants exposed to higher levels of oxygen develop more serious cases of lung disease [23]. Hyperoxia has been found to induce inflammatory responses, which disrupt alveolarization [24], the oxygen toxicity appears to be prompted by reactive oxygen species [25]. Similarly, mechanical ventilation also promotes a proinflammatory reaction in the preterm lung [26], specifically, the proinflammatory reaction was prompted by volutrauma caused by high tidal volumes [27], and atelectrauma caused by insufficient positive end-expiratory pressures (PEEP) [28].

1.3.2 Bronchopulmonary dysplasia treatment

Considering that BPD has severe long-term consequences, not only causing diminished lung function, but also potentially causes early onset of chronic obstructive pulmonary disease (COPD) in adults, an ideal therapy regimen is imperative. Furthermore, BPD has been associated with higher rates of cognitive impairment and language delay [29, 30]. Therefore, an ideal treatment of the preterm infant is required, which currently consists of optimal ventilation and oxygen therapy, postnatal and antenatal corticosteroids, Caffeine, Vitamin A and surfactant therapy [1].

Keeping in mind that mechanical ventilation is a major risk factor for BPD, lung protective ventilation, although challenging to apply successfully, continues to be an important method. Latest studies suggest that volume-targeted ventilation is superior to traditional pressure-limited ventilation in reducing mortality and BPD [31]. On the other hand, optimal oxygen therapy is subject to current research, and is therefore yet to be

determined. However, studies have been made to compare a lower target range of oxygen saturation (85-89%) and a higher range of oxygen saturation (90-95%) as oxygen treatment, showing that a lower target range of oxygen saturation increases overall mortality, yet decreases the incidence of BPD [32]. Women at risk for giving birth prematurely are treated with antenatal corticosteroids to decrease mortality and respiratory distress syndrome (RDS) in the preterm infant. Even though there was no significant effect on the incidence of BPD, the incidence of RDS was reduced by around 50% [3]. The missing effect on the rate of BPD can be explained by the increased survival of infants at risk of BPD. The same explanation can be given as to why surfactant therapy does not decrease the incidence of BPD [33]. However, corticosteroids are not only applied before birth, but also postnatal. Short-term corticosteroid therapy enhances lung function and suppresses pulmonary inflammation [34]. Therefore, postnatal corticosteroids are an important medication to decrease the incidence of BPD, although side effects include cerebral palsy and intestinal perforation if given at ≤7 days postnatal [35]. Furthermore, BPD treatment also consists of caffeine, which causes the number of apnoeic attacks to drop [36] and is known to curb the rate of BPD in VLBW infants, and is therefore the drug of choice to prevent BPD in VLBW infants [37]. Finally, supplementing high doses of Vitamin A has shown a small, but statistically significant reduction of BPD in VLBW infants [38] and is therefore considered a therapy option to prevent BPD. Although stem cell treatment is yet to be implemented into BPD therapy, several studies hint at its potential, suggesting that stem cells avert and repair hyperoxia induced lung damage in rodents [39]. For that reason, stem cells, combined with conventional therapy options, may play a significant role in the future treatment of BPD.

1.4 MicroRNA biology

MicroRNAs (miRNAs) are endogenous, approximately 22 nucleotides short, single-stranded RNA molecules that regulate gene expression by binding at the 3'-untranslated region (UTR) of the target mRNAs. This process is mediated by the RNA-induced silencing complex (RISC) [40]. Since their discovery, almost 2000 miRNAs have been described in humans, which are able to target >60% of protein-coding genes in humans [41]. One miRNA can target the expression of more than one gene, but likewise, one gene can be regulated by several miRNAs [42]. Research suggest regulatory roles for miRNAs in many different biological processes in animals, plants and fungi [40], the most important ones being early development and oncogenesis [43, 44].

1.4.1 MicroRNA biogenesis and function

In the first step of miRNA biogenesis, primary miRNA (pri-miRNA) is transcribed in the nucleus by either RNA polymerase II or RNA polymerase III [45, 46] (**Fig. 4**). Primary transcripts of miRNA can be edited by adenosine deaminases acting on RNA (ADARs) by changing adenosine into inosine, thus possibly changing their sequence, and affecting their target specificity [47]. In the next step, the pri-miRNA is cleaved by the RNase III enzyme Drosha and the DiGeorge critical region (DGCR) 8, resulting in an approximately 70-100-nucleotide long stem-loop structure, called pre-miRNA [48]. While Drosha appears to cut the pri-miRNA, the role of DGCR 8 is to determine the correct cleavage site [49].

The pre-miRNA is then transported from the nucleus into the cytoplasm by joint efforts of Exportin (XPO) 5 and Ran-GTP [50]. XPO5 identifies the pre-miRNA independently from its sequence by a specific length of the stem and the 3' overhang, in order to only export correctly cleaved miRNAs [51].

In the cytoplasm, the exported pre-miRNA is further cleaved by RNAse III enzyme Dicer into a miRNA duplex. Dicer is supported by RNA-binding domain proteins Tar RNA binding protein (TRBP), protein activator of PKR (PACT). Although TRBP and PACT are not essential to the reaction, they seem to facilitate the reaction and speed up the cleavage [52, 53]. After cleavage by Dicer, the miRNA duplex is unwound by a helicase [54], which leaves two strands. The strand with the least stable base pair at its 5' end is recruited by Ago 1 or 2 and then integrated into the RISC, the other is degraded [55], therefore concluding miRNA biogenesis. Although the pathway described is thought to be the canonical miRNA-processing pathway, many studies have revealed miRNA-specific differences, which in turn could potentially reveal many regulatory options to process miRNAs [10].

The RISC, consisting of the mature miRNA and Ago proteins, is the executive body of the miRNA, which functions by matching with its complementary target mRNA and then interacting with it. There are different mechanisms, by which the RISC is able to reduce mRNA translation and therefore gene expression: If the complementarity of the mRNA to the miRNA is sufficient, the mRNA is degraded by ubiquitination, thus inhibiting translation of the mRNA. If the complementarity of the mRNA to the miRNA is rather

imperfect, the RISC resorts to translational repression and sequestration from the translational complex, by mechanisms that are yet to be fully understood [56]. This therefore leads to reduced protein levels and has far reaching consequences on the cells.

By reducing gene expression of many proteins, miRNA are indicated to play crucial roles in for example early development [57], proliferation [58] and apoptosis [59]. Because miRNAs regulate such vital processes, altered miRNA expression has been linked to various diseases, such as cancer. miRNAs can act as oncogenes and tumor suppressors, implicating their future importance in diagnostics and treatment of cancer [60]. Because miRNAs are differently expressed in different tissues, they could alter gene expression in a way that allows for specific protein levels in different cell types [40].

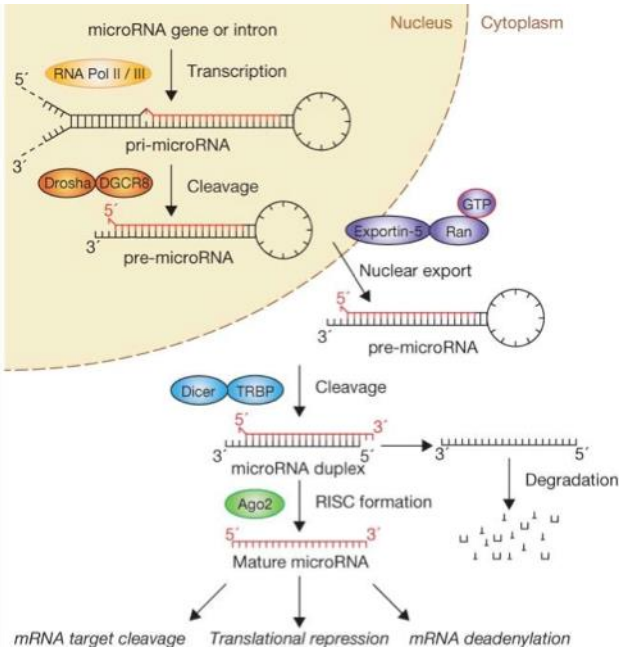

Figure 4. MicroRNA biogenesis. The canonical pathway of microRNA (miRNA) synthesis in nucleus and cytoplasm is shown. The pri-miRNA is transcribed by RNA-polymerase II or III, and then cleaved by the Drosha-DiGeorge syndrome critical region (DGCR) 8 complex to form a pre-miRNA. In the following step, the pre-miRNA is exported from the nucleus into the cytoplasm by Exportin-5, where it is once more cleaved by Dicer, leaving a miRNA duplex. This duplex is then unwound by a helicase, and finally the mature miRNA is integrated into the RNA-induced silencing complex (RISC). Image from [10].

1.4.2 MicroRNA in lung development

Despite the fact that very little is known about miRNA function, they are strongly implicated in the development of many organs, including the heart [61] the nervous system [62] and haematopoiesis [63]. The first study to have shown that miRNAs may also be involved lung development, used Dicer knockout mice, which exhibited aberrant alveolarization, abnormal epithelial branching and apoptosis [64]. Further evidence for miRNA involvement in lung development is that several miRNAs were found to be upregulated in foetal lungs compared to adult lungs [65]. Furthermore, mice lacking Ago2, a crucial component of the RISC, die before birth. This study also showed that Ago1 and Ago2 were expressed in specific locations in the lung, all in all suggesting miRNA significance in lung development [66]. Additional evidence to miRNA involvement in lung development is that the expression of one of the largest miRNA clusters, miR-17-92, is decreased as lung development progresses [67]. Over-expressing the miR-17-92 cluster resulted in highly proliferative and undifferentiated epithelial cells of the lung [68], features that are also typical for cancer. Interestingly, miR-17-92 is overexpressed in human lung cancer [69].

So therefore, efforts have been made to investigate the role of miRNAs in lung diseases, such as BPD. Using a micro-array analysis, Bhaskaran and colleagues identified miRNAs in the lung that were altered after hyperoxia exposure. The microRNAs that were downregulated were miR-342, miR-335, miR-150, miR-126* and miR-151*, and the upregulated miRNAs were miR-21 and miR-34a [4]. Moreover, it was discovered that the application of antagomiR-489 to block miR-489 improved lung structure [70] In conclusion, the evidence supporting miRNA involvement in both lung development and disease suggests vast potential for treatment options in the future and makes miRNAs such a compelling field of research.

1.4.3 The miR-34 family

In the aforementioned study by Bhaskaran and colleagues, amongst others, miR-34a was upregulated at E21, P6 and P14 after hyperoxia exposure [4], therefore becoming an interesting target for BPD research. The highly conserved miR-34 family consists of three members: miR-34a, miR-34b and miR-34c. In mice, miR-34a is located on chromosome (Chr) 4, miR-34b and miR-34c are located on Chr 9, albeit in humans, miR-34a is found on Chr 1, miR-34b and miR-34c on Chr 11 [71] (**Fig. 5**). miR-34a is expressed

ubiquitously in mice, but its highest levels of expression are found in the brain, while miR-34b and miR-34c are mainly expressed in the lung. However, in total, miR-34a is expressed at higher levels than miR-34b and miR-34c [72].

Current research suggests that the miR-34 family is involved in cell proliferation and apoptosis since their targets are, for example, factors required for G1/S transition (c-MYC [73]) and anti-apoptotic proteins (Bcl2 [74], SIRT1 [75]), inducing cell cycle arrest and apoptosis in tumour cells. Furthermore, overexpression of miR-34a causes downregulation PDGFRα and PDGFRβ in non-small cellular lung cancer (NSCLC) cell lines [76] Additionally, it was reported that miR-34a is a direct transcriptional target of p53, a transcriptional factor that induces apoptosis and growth arrest. These reports therefore suggest that miR-34a deregulation is a factor to cancer development [43]. Furthermore, miR-34a appears to also play an important role in cardiac ageing and function. Research shows that not only miR-34a was expressed at a higher level in the heart of aged mice than in the heart of young mice, but also that miR-34a inhibition improves recovery of cardiac function after acute myocardial infarction [77].

The heavy involvement of miR-34a in cancer development is hard to overlook, given the evidence. However, cell proliferation and apoptosis are crucial features of not only cancer, but also organogenesis, thus indicating an important, yet still unknown role for miR-34a in lung development and therefore BPD.

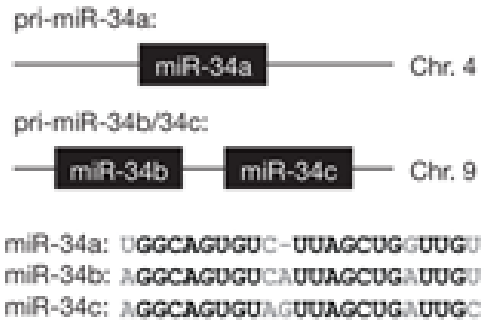

Figure 5. Genomic organization of the miR-34 family in mice. Above: microRNA (miR)-34a is located on Chromosome (Chr) 4, whereas miR-34b and miR-34c are located on Chr 9. Below: Comparison of the sequences of the miR-34 family, in which the common nucleotides are highlighted. Image adapted from [77]

1.5 The platelet-derived growth factor receptors

As previously mentioned, miR-34a was shown to target PDGFRα and PDGFRβ. In this study, miR-34a was revealed to target the PDGFRα and PDGFRβ 3' UTRs and miR-34a expression was inversely related to PDGFRα and PDGFRβ expression [76], thus presenting a clear connection between miR-34a and PDGFR.

PDGFRs are tyrosine kinase receptor molecules that are located on the cell surface. There are two chains: α and β, which are able to form 3 different dimeric receptors upon activation by their ligand: PDGFRαα, PDGFRαβ and PDGFRββ [78]. Their also dimeric ligands are PDGF-AA, PDGF-AB, PDGF-BB, PDGF-CC and PDGF-DD. Each ligand binds to the receptors differently (**Fig. 6**). PDGFA exclusively binds to PDGFRα [79], PDGFD mostly binds to PDGFRβ [80], and PDGFB binds to all receptors, therefore it is the most potent ligand of the PDGF-family [79]. Following dimerization and autophosphorylation, the PDGFRs activate downstream signalling molecules including Growth factor receptor-bound protein (Grb) 2, which in a complex with son of sevenless (Sos) 1 activates the Ras and the extracellular signal-regulated kinase (ERK) pathway. Furthermore, PDGFR phosphorylation activates phospholipase C, which then leads to an activation of protein kinase C [81]. Additionally, phosphoinositide-3-kinase (PI3K) is activated, which activates the AKT kinase, also known as protein kinase B [82].

PDGFR regulates proliferation, migration and differentiation of cells [83], moreover it has been shown that PDGFR expression induces oncogenic transformation [84]. These findings indicate an important role for PDGFR in cancer and lung development, and therefore BPD. PDGFR downregulation mediated by miR-34a induced apoptosis and reduced tumourgenesis in lung cancer [76], highlighting the importance of both PDGFR and miR-34a in cancer. Additionally, it was shown, that PDGFR and transforming growth factor (TGF) β, an anti-oncogenic protein, interact closely with one another [85]. The importance of PDGF-signalling in lung development was demonstrated by studying PDGF-AA null mice, whose lungs showed emphysema and failure to form alveoli by secondary septation [86]. Further examination by the same group came to the conclusion that PDGF-signalling is crucial for late lung development, but not early branching morphogenesis [87], suggesting PDGFR may play a role in alveologenesis. Further evidence is shown by a study that demonstrated PDGFRα expressing cells were located

at the alveolar entry ring [88]. Furthermore, in BPD research, Popova and colleagues showed that PDGFR expression was reduced in human BPD [89].

Therefore PDGF-signalling appears to be a crucial factor, not only in cancer, but also in lung development and thus appears to be an important target for further BPD research.

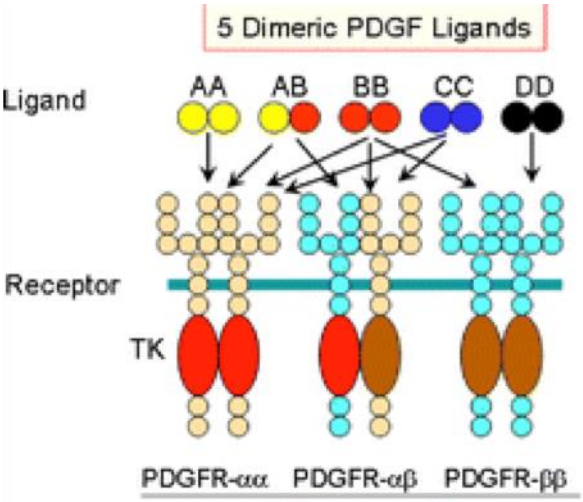

Figure 6. The PDGF ligands and their receptors. The homo- or heterodimeric ligands each bind differently to the dimeric receptors, which also form hetero- or homo-dimers. TK: Tyrosin kinase. Image adapted from [90**]**

2 Hypothesis and thesis objective

Even though considered a rare disease, many preterm infants develop BPD. However, although much progress has been made in controlling the disease and reducing long- term effects, a definitive cure is yet to be found. Therefore, further research regarding BPD and late lung development is required.

Amongst other factors, fibroblast migration is implied to be a defining feature of alveolar septation [11], and its deterioration is an essential trait of BPD. Previous studies already established the importance of fibroblasts and PDGFRα in alveolar septation. It was shown, that PDGF-A null mice developed lung emphysema, due to failure of alveolar septation. Furthermore, α-smooth muscle actin (α-sma), the marker for the contractile elements of myofibroblasts and the parenchymal elastin were strongly reduced in PDGF-A null mice, suggesting, firstly that the parenchymal elastin is produced by the myofibroblasts in the lung and secondly, that PDGF-A is involved in myofibroblast differentiation [86]. A study by Bhaskaran and colleagues demonstrated that miR-34a was upregulated in lungs treated with high levels of oxygen, suggesting a role in BPD pathogenesis [4]. Furthermore, it was shown that miR-34a downregulates PDGFRα and PDGFRβ by targeting its 3' UTR, thus linking miR-34a and the PDGF receptors [76]. However, it is yet to be demonstrated how miR-34a regulates fibroblast migration, therefore the hypothesis was constructed that miR-34a regulates mouse lung fibroblast migration by modulating PDGF signalling.

The objective of this thesis is to investigate if miR-34a influences fibroblast migration by downregulating PDGFRα and PDGFRβ. To this end, a series of in vitro experiments were carried out, in which mouse lung fibroblasts were transfected with a miR-34a mimic to investigate its effect on PDGFRα and PDGFRβ, their downstream signalling and the effect on fibroblast migration.

3 Materials and methods

3.1 Materials

3.1.1 Technical equipment

Material	Manufacturer (production site)
-20 °C freezer	Gram Commercial A/S (Vojens, Denmark)
-80 °C freezer	New Brunswick Scientific (Enfield, USA)
+4 °C refrigerator, Comfort Nofrost	Liebherr (Bieberrach, Germany)
Airflow control hood	Vinitex (Sint Oedenrode, Netherlands)
Cell counter, Countess™ automated cell counter	Invitrogen (Eugene, USA)
Centrifuge, Heraeus Fresco 17	Thermo-Scientific (Waltham, USA)
Centrifuge, Heraeus Multifuge 3 S-R	Thermo-Scientific (Waltham, USA)
Incubator, CO_2 incubator HERAcell 150i	Thermo-Scientific (Waltham, USA)
Incubator, Heraeus Function Line	Thermo-Scientific (Waltham, USA)
Liquid nitrogen container	Cryotherm (Kirchen, Germany)
Luminescence image Analyzer, Imagequant LAS-4000	General Electric (Fairfield, USA)
Microplate reader, Versa Max	Molecular Devices (Sunnyvale, USA)
Microscope, Leica DMIL	Leica (Solms, Germany)
Microscope with camera, Leica DMI 3000 B	Leica (Solms, Germany)
O_2-Sensor	Biospherix (Lacona, USA)
PCR machine, Step One Plus Real time PCR system	Thermo-Scientific (Waltham, USA)

pH-Meter, pH211 microprocessor pH-Meter	Hanna (Kehl, Germany)
Pipette, Pipet-Boy Acu 2	Integra (Fernwald, Germany)
Power supply, Power Pac HC	Biorad (Hercules, USA)
Real-time qPCR-machine, Peqstar	Peqlab (Erlangen, Germany)
Roller mixer	Stuart (Stone, UK)
Sample mixer	Thermo-Scientific (Waltham, USA)
Scale	Kern (Balingen, Germany)
Shaker, Unimax 2010	Heidolph (Schwabenbach, Germany)
Spectrophotometer, Nandrop ND1000	Peqlab (Erlangen, Germany)
Suction pump, Automatic vacuum-security suction system	Ditabis (Pforzheim, Germany)
Thermo shaker	Ditabis (Pforzheim, Germany)
Tissue culture hood, Safe 2020.12	Thermo-Scientific (Waltham, USA)
Vortex-machine, Genius 3	IKA (Staufen, Germany)
Water bath, VWB 12	VWR (Leuven, Belgium)

3.1.2 Chemicals

Materials	**Manufacturer (production site)**
Acrylamid, Rotiphorese Gel 30 acrylamid	Roth (Karlsuhe, Germany)
Bradford dye	Bio-rad (Hercules, USA)
Bromphenol blue sodium salt	Sigma-Aldrich (St. Louis, USA)
Bovine serum albumin (BSA)	Invitrogen (Carlsbad, USA)
Buffer solution, pH 4,7,10	Hanna (Kehl, Germany)
Chloroform, 99%	Sigma-Aldrich (St. Louis, USA)

Complete	Roche (Basel, Schweiz)
Dimethylsulfoxide (DMSO)	Sigma-Aldrich (St. Louis, USA)
Dithiothreitol (DTT)	Sigma-Aldrich (St. Louis, USA)
Ethylenediaminetetraacetic acid (EDTA)	Promega (Madison, USA)
Ethylene glycol tetraacetic acid (EGTA)	Sigma-Aldrich (St. Louis, USA)
Ethanol, 70% and 100%	Roth (Karlsruhe, Germany)
Glycerol, anhydrous	Merck (Hohenbrunn, Germany)
Glycin	Roth (Karlsruhe, Germany)
Hydrochloric acid (HCL) 25%	Roth (Karlsruhe, Germany)
Marker, Precision Plus Protein Dual Color Standarts	Bio-rad (Hercules, USA)
Maximum Sensitivity Substrate, SuperSignal® West Femto	Thermo-Scientific (Waltham, USA)
Mercaptoethanol, 98%	Sigma-Aldrich (St. Louis, USA)
Methanol, 99.90%	Roth (Karlsruhe, Germany)
Milk powder	Roth (Karlsruhe, Germany)
Sodium chloride (NaCl)	Roth (Karlsruhe, Germany)
Sodiumhydroxide solution (NaOH)	Merck (Hohenbrunn, Germany)
O_2, 95%	Westfalen (Münster, Germany)
Sodium dodecyl sulfate (SDS)	Roth (Karlsruhe, Germany)
N,N,N´,N´-Tetramethylethylenediamine (TEMED)	Sigma-Aldrich (St. Louis, USA)
Tris Buffer	Roth (Karlsruhe, Germany)
Trypan-Blue solution	Fluka (St. Gallen, Switzerland)
Tween 20	Sigma-Aldrich (St. Louis, USA)
Natriumorthovanadate	Sigma-Aldrich (St. Louis, USA)

3.1.3 Lab commodities

Material	Manufacturer (production site)
6- well cell culture plate	Greiner-bio-one (Frickenhausen, Germany)
Countess™ cell counting chamber slide	Invitrogen (Carlsbad, USA)
Cell culture dishes	Greiner-bio-one (Frickenhausen, Germany)
Disposable glass pasteur pipettes	VWR (Leuven, Belgium)
Electronic pipettes, Xplorer 15-300 µl	Eppendorf (Hamburg, Germany)
Filter tip, Biosphere® 0.5-10 µl, 2-20 µl, 2-100 µl, 200 µl, 100-1000 µl	Sarstedt (Nümbrecht, Germany)
Freezing container, Nalgene Cryo 1 °C	Thermo-Scientific (Waltham, USA)
Cryovials	Greiner-bio-one (Frickenhausen, Germany)
Nitrile gloves, size M	VWR (Leuven, Belgium)
Perfusor syringe, 50 ml	Braun (Melsungen, Germany)
Pipettes, 10-1000 µl range	Eppendorf (Hamburg, Germany)
Reagent tubes, Safe Seal micro tube (0.5 ml and 1.5 ml)	Sarstedt (Nümbrecht, Germany)
Reagent tubes, 25 ml and 50 ml, blue cap	Greiner-bio-one (Frickenhausen, Germany)
Serological pipette, sterile, Cellstar® 5 ml, 10 ml, 25 ml, 50 ml	Greiner-bio-one (Frickenhausen, Germany)
Syringe driven filter unit, 33 mm, 0.22 µm pore size	Millex (Tullagreen, Ireland)
TC-flask, T75	Sarstedt (Nümbrecht, Germany)

3.1.4 Cell culture

Material	Manufacturer (production site)
Dulbecco's Phosphate buffered saline (PBS)	Sigma-Aldrich (St. Louis, USA)
Eagle's minimal essential medium (EMEM)	ATCC (Manassas, USA)
Foetal bovine serum (FBS)	Lonza (Walkersville, USA)
Lipofectamine® 2000	Invitrogen (Carlsbad, USA)
MiScript miRNA mimic kit	Qiagen (Hilden, Germany)
OptiMEM®	Gibco (New York, USA)
Trypsin-EDTA-solution	Sigma-Aldrich (St. Louis, USA)

3.1.5 Cell-types

Material	Manufacturer (production site)
Mouse Lung fibroblasts (MLg), Cell-line (MLg 2908) (CCL-206)	ATCC (Manassas, USA)

3.1.6 Antibodies

Table 1. Overview of all antibodies used in alphabetical order.

Antibodies	Host	Dilution	Catalogue Number	Manufacturer (production site)
Anti-AKT	rabbit	1:1000	9272	Cell Signalling Technology (Danvers, USA)
Anti-p44/42 MAPK (ERK1/2)	rabbit	1:1000	9102	Cell Signalling Technology (Danvers, USA)

Anti-PDGFRα	rabbit	1:1000	3164	Cell Signalling Technology (Danvers, USA)
Anti-PDGFRβ	rabbit	1:1000	C82A3	Cell Signalling Technology (Danvers, USA)
Anti-Phospho-AKT	rabbit	1:500	9271	Cell Signalling Technology (Danvers, USA)
Anti-Phospho-p44/42 MAPK (ERK1/2)	rabbit	1:500	9101	Cell Signalling Technology (Danvers, USA)
Anti-βactin	rabbit	1:1000	4967	Cell Signalling Technology (Danvers, USA)
Secondary antibodies	rabbit	1:3000		Santa Cruz (Heidelberg, Germany)

3.1.7 Proteins

Material	**Manufacturer (production site)**
PDGFA, *mouse*, recombinant	Creative Biomart (Shirley, USA)
PDGFB, *mouse*, recombinant	Creative Biomart (Shirley, USA)
PDGFD, *E. coli*, recombinant	Mybiosource (San Diego, USA)

3.1.8 Western blot

Material	**Manufacturer (production site)**
Cell scraper	Sarstedt (Nümbrecht, Germany)
Chromatography paper, 3 mm	GE Healthcare UK, Little Chalfont
Mini-Protean® Tetra Cell	Bio-rad (Hercules,USA)
Mini-Trans-Blot® Cell	Bio-rad (Hercules,USA)

Nitrocellulose membrane, 0.2 µm	Bio-rad (Hercules,USA)
Tissue culture plate 96 well	Sarstedt (Nümbrecht, Germany)

3.1.9 Migration assay

Material	**Manufacturer (production site)**
Cell culture flasks, 25 cm^3 50 ml	Greiner-bio-one (Frickenhausen, Germany)
Cell insert, 30 µ-dish 35 mm, low, culture insert	Ibidi (Planegg, Germany)
Grid plates, 60 µ-dish, 35 mm, low Grid 500	Ibidi (Planegg, Germany)
Improved Neubauer Chamber	Marienfeld superior (Lauda, Germany)
Tweezers	Martin (Solingen, Germany)

3.1.10 Real-time qPCR

Material	**Manufacturer (production site)**
Micro Amp Fast 96-Well Reaction Plate (0.1 ml)	Thermo-Scientific (Waltham, USA)
miRNeasy Mini kit (50)	Qiagen (Hilden, Germany)
MiScript II RT kit	Qiagen (Hilden, Germany)
miScript PCR kit, SYBR Green 200	Qiagen (Hilden, Germany)
Qiazol Lysis reagent	Qiagen (Hilden, Germany)

3.1.11 Primers

Gene	Catalogue number	Manufacturer (production site)
miR-34a-5p	MS00001428	Qiagen (Hilden, Germany)
miR-34a-5p	MS00007910	Qiagen (Hilden, Germany)
miR-34a-5p	MS00001442	Qiagen (Hilden, Germany)
RNU6-2	MS00033740	Qiagen (Hilden, Germany)

3.1.12 Software

Material	Manufacturer (production site)
Graphpad Prism, 6.02	Graphpad Software, (Lajolla, USA)
Image J	General Electric (Fairfield, USA)
Leica Application Suite, V3	Leica (Solms, Germany)
Microsoft Excel	Microsoft (Redmond, USA)
Nanodrop software, ND1000 V3.3.0	Peqlab (Erlangen, Germany)
	Thermo-Scientific (Waltham, USA)
Real Time software, Step One Software	

3.2 Methods

3.2.1 Cell-culture

3.2.1.1 Thawing fibroblasts and changing medium

Foetal bovine serum (FBS), filtered through a syringe driven filter unit with 0.22 µm pore size, was added to Eagle's minimum essential medium (EMEM), so that the medium

contained 10% (v/v) FBS (EMEM complete medium). A cell culture flask was filled with 10 ml of EMEM complete medium and incubated at 37 °C and at 5% CO_2 for 15 min. In the meantime, an aliquot of fibroblasts was taken from the liquid nitrogen storage at -210 °C and was thawed at 37 °C. Once thawed, fibroblasts were transferred into the flask and then incubated at 37 °C and at 5% CO_2. After 24 h the medium was replaced with fresh medium. Under the tissue culture hood the medium in the cell culture flask was aspirated using a glass pasteur pipette connected to a suction pump. Then, 12 ml of EMEM complete medium was transferred into the cell culture flask and placed at 37 °C and at 5% CO_2.

3.2.1.2 Cell passage and counting cells

Fibroblasts were washed with 5 ml of 1× PBS, and then incubated with 3 ml of trypsin at 37°C for 3 min to detach the fibroblasts from the flask. The function of the trypsin was inhibited by adding 7 ml of EMEM complete medium to add up to a total of 10 ml in the flask. Then, 45 µl of trypan-blue and 5 µl of the cell-suspension (dilution of 1:10) were mixed in a 1.5 ml tube, so that 10 µl could be pipetted onto the cell-counting slide, to count the cells. To determine the volume of cell suspension per flask, the following was calculated:

Calculations: Total cells in reagent tube = n cells/ml × 5 × 10 ml, where n is number of cells in 1 ml, determined by counting cells.

$[c]_{10\ ml}$ (cells/ml) = Total cells/10 ml, where $[c]_{10\ ml}$ is the concentration of cells in the flask

Volume/flask (ml) = Cells needed per flask × $1/[c]_{10\ ml}$

The fibroblasts were split over three cell-culture flasks (T75) for an approximately 70% confluent monolayer in three days. The cell culture flasks were filled up with medium to a 12 ml total and were incubated at 37 °C and 5% CO_2.

3.2.1.3 Seeding cells into 6-well plates

Once the fibroblasts had reached an approximately 70% confluent monolayer the fibroblasts were ready to be seeded into 6-well cell culture plates. The cells were detached as described in **3.2.1.2**. In order to calculate the volume of cell suspension per well, the following calculation were made:

Calculations: Total cells in reagent tube = *n* cells/ml × 5 × 10 ml, where *n* is number of cells in 1 ml, determined by counting cells.

$[c]_{10\ ml}$ (cells/ml) = Total cells/10 ml, where $[c]_{10\ ml}$ is the concentration of cells in the flask

$[c]_{50\ ml}$ (cells/ml)= $[c]_{10\ ml}$/5, where $[c]_{50\ ml}$ is the concentration of cells in the flask, after filling the tube up to 50 ml, to dilute the cell suspension.

Volume/well (ml) = Cells needed per well × 1/$[c]_{10\ ml}$

After $[c]_{10\ ml}$ was calculated, 40 ml of media were added to the suspension, making it a 1:50 dilution. The suspension was mixed thoroughly, but carefully. Into each well 600,000 fibroblasts were seeded. The 6-well cell culture plates were placed in the incubator at 37 °C and at 5% CO_2. After 24 h to 48 h the fibroblasts would have formed an approximately 70% confluent monolayer.

3.2.2 Hyperoxia exposure

Fibroblasts were seeded into four separate 6-well plates as described in **3.2.1.2**. The fibroblasts were seeded into the wells as shown in **figure 7**. The cells were incubated until approximately 70% confluence was reached, and then the fibroblast cell cycles were synchronised by starving the cells in 0% (v/v) FBS EMEM for 12 h. After starvation, the medium was replaced with EMEM complete medium and the fibroblasts were incubated in either 85% oxygen (O_2) or 21% O_2 for either 24 h or 48 h.

3.2.3 Real-time quantitative PCR analysis

3.2.3.1 RNA-isolation

To harvest the fibroblasts, to each well 200 µl of QIAzol lysis reagent was added. After transferring the fibroblasts into different tubes, RNA was extracted using a miRNeasy® Mini kit following the manufacturer's instructions. To measure the RNA concentration of the samples, a spectrophotometer of the type Nanodrop ND1000 was used. Once the RNA concentration for each sample was determined, the exact volume of each sample containing 0.2 µg of RNA was calculated, using the following formula:

Calculations: Volume/sample (µl) = 0.2 µg × (1/[c]), where [c] is the measured concentration by spectrophotometer of each sample.

The samples containing 0.2 µg of RNA were then used to synthesize cDNA.

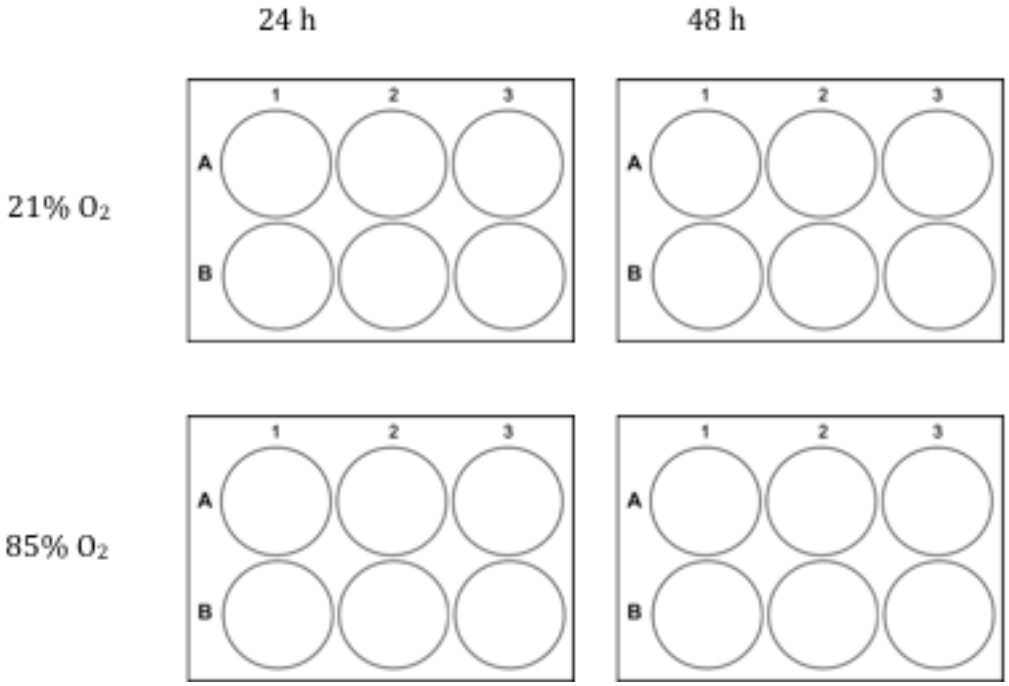

Figure 7. Hyperoxia exposure. Fibroblasts are seeded into the wells of each 6-well plate. The fibroblasts exposed to 21% O2 are the control group, and were incubated for 24 h or 48 h. The fibroblasts exposed to 85% O2 were also incubated for 24 h or 48 h.

3.2.3.2 cDNA-synthesis

Firstly, the amount of RNAse-free water needed was calculated, using the following formula:

20 µl - 8 µl - *X* µl = RNAse-free water (µl), where 20 µl is the total amount for each well, 8 µl is the volume of the mastermix and *X* µl is the volume of the sample containing 0.2 µg RNA.

To create the mastermix, each sample required:

a. 4 µl of 5× HiSpec Buffer
b. 2 µl of 10× nucleic mix
c. 2 µl of Reverse Transcriptase

All the reagents listed above were provided in the miScript II RT kit

At this point, the calculated amount of RNAse-free water, the 0.2 µg of RNA and 8 µl of the master mix were added to a 0.5 µl tube. Each micro tube was both mixed and

centrifuged briefly before it was placed inside the cDNA-machine peqstar 2x Gradient to perform the reverse-transcription (RT) PCR. When the RT-PCR had finished, each sample was diluted with 40 µl of RNAse-free water.

3.2.3.3 Real-time quantitative PCR and processing data

For the real-time qPCR the miScript SYBR Green PCR kit and the Step One Plus Real Time PCR system were used.

First, the reagents were mixed according the following protocol. For each sample the following was required:

a. 12.5 µl of 2× Quantitect SYBR Green PCR Master mix
b. 2.5 µl of 10× miScript Universal Primer
c. 5.0 µl of RNAse-free water

All the reagents listed above were provided in the miScript SYBR Green PCR kit.

In the following step, 20 µl of the reaction mix were pipetted into each well of a Micro Amp Fast 96-Well Reaction Plate (0.1 ml). Then, 2.5 µl of cDNA and 2.5 µl of primer Assay were added. After selecting Quantstudio™ Real-Time PCR Software, and setting up the real-time qPCR, the 96-well plate was placed inside the machine and the real-time qPCR was started.

After the real-time qPCR was completed, the data was exported into Microsoft Excel, and the ΔC_T of each gene of interest were calculated applying the following formula:

Housekeeping C_T mean – gene of Interest C_T mean = ΔC_T, where C_T is Cycle Threshold.

The data then was exported into the Prism Graph Pad software to be analysed and to be plotted in a graph.

3.2.4 Transfection

Before transfection, MLg fibroblasts were seeded into 6-well plates as described in **3.2.1.2**. The transfection reagent used for the MLg cell line was Lipofectamine® 2000, which was combined with scrambled microRNA (SCR) ([c] 20 µM) and miR-34a mimic (MIM34a) ([c] 20 µM) at a ratio of 2:1. In this particular case, 4 µl of SCR and 4 µl of MIM34a each were combined with 8 µl of Lipofectamine® 2000 and incubated at room

temperature to form transfection complexes for 20 min. Together with 1000 µl transfection medium OptiMEM™, the transfection complexes were then pipetted onto the fibroblasts (**Fig. 8**), and were incubated at 37 °C and at 5% CO_2 for 4-6 h in order to allow the transfection complexes to enter the cells. After 4-6 h, OptiMEM™ was replaced with EMEM complete medium. Protein isolation was performed 24 h after transfection.

Calculations: $[c]_{Stock}$ 20 µM of SCR or MIM34a × 4 µl = 80 µM of SCR or MIM34a

$[c]_{Transfection}$ = 80 µM/1000 µl OptiMEM = 80 nM of SCR or MIM34a on each sample of fibroblasts.

3.2.5 Fibroblast stimulation

The MLg fibroblasts were seeded into 6-well plates as described in **3.2.1.2** and transfected as shown in **3.2.4**. After 4-6 h of transfection, the SCR and MIM34a transfected MLg fibroblasts and 3 of the 6 non-transfected wells were stimulated **(Fig. 9).** Depending on which stimulant was used, different concentrations of the stimulant were added to the fibroblasts [80, 90]. If stimulating the fibroblasts with PDGFA, 80 ng/ml were used, if stimulating with PDGFB, 40 ng/ml were used and if stimulating with PDGFD, 160 ng/ml were used to stimulate the MLg fibroblasts. After the stimulant was diluted using EMEM complete medium and then pipetted onto the MLg fibroblasts, the fibroblasts were incubated for 30 min prior to protein isolation.

3.2.6 Protein isolation, Bradfordassay and sample preparation

First, the lysis buffer containing 20 mM tris (pH 7.5), 150 mM NaCl, 1 mM EDTA, 1 mM EGTA and 0.5% NP-40, diluted with dH_2O, was supplemented with 1 mM sodium orthovanadate and 1 mM complete™ protease inhibitor cocktail. Then, 100 µl of lysis buffer were used to harvest the fibroblasts employing a cell scraper. In the next step, the fibroblasts were incubated on ice at approximately 4 °C for 30 min, vortexing every ten

Figure 8. Model for fibroblast transfection, without stimulation. Mouse Lung (MLg) fibroblasts were seeded into each well. After reaching 70% confluence, the fibroblasts are treated with either 80nm scrambled microRNA (SCR) or micro-RNA 34a mimic (MIM34a) as indicated in the figure. Mock: Cells treated with Lipofectamine only.

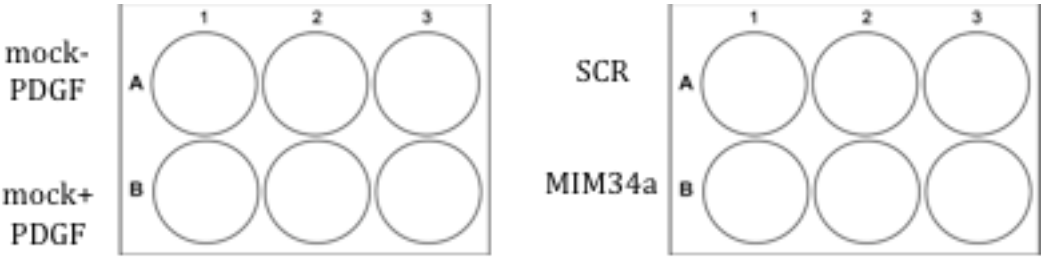

Figure 9. Model for fibroblast transfection, with stimulation. Mouse Lung (MLg) fibroblasts were seeded into each well. The fibroblasts are treated with either 80nm scrambled microRNA (SCR) or micro-RNA 34a mimic (MIM34a) as indicated in the figure. Mock-PDGF: Cells treated with Lipofectamine only, mock+PDGF: Cells treated with Lipofectamine and stimulated with PDGF.

min. After that, the cells were centrifuged at 13,249.6 × *g* for 15 min at 4 °C. After centrifuging, the supernatant, containing the proteins, was collected to perform a Bradford assay to measure protein concentration. The Bradford assay was performed using a micro-plate reader measuring the absorbance at 570 nm wavelengths. The protein concentrations from the samples were then derived from a bovine serum albumine (BSA) standard curve. The concentrations of the BSA standard curve solutions were 0.05 µg/µl, 0.1 µg/µl, 0.2 µg/µl, 0.3 µg/µl, 0.4 µg/µl and 0.5 µg/µl. Therefore, 10 µl of each BSA standard curve solution, distilled H_2O (dH_2O), lysis buffer and protein samples were pipetted into a 96-well plate (**table 2**). After adding 200 µl of Quick Start ™ Bradford dye reagent to each well and incubating the plate for 5 min, the protein concentration of the samples was determined. Then, the formula shown below was used to calculate the µl per well in order to fill each well with the same amount of protein.

Calculations: Load/well (µg) × 1 µl/[c] $_{sample}$

For example: Given, that the load/well is 40 µg and the protein concentration is 1 µg/µl

40 µg × 1 µl/1 µg/µl = 40 µl/well

The proteins were combined 1:3 with a 5× Laemli buffer containing 100 mM tris (pH 6.8), 4% Sodiumhydroxide solution (SDS), 0.2% bromphenol blue and 20% glycerol and 100µM Dithiothreitol (DTT). Before loading into acrylamide gels, the proteins were denatured at 95 °C for 10 min.

3.2.6.1 Casting the gel, electrophoresis and Transfer

The denatured proteins were loaded into 8% or 10% (v/v) acrylamide gels. To cast the acrylamide gels, the Mini-Protean® Tetra Cell kit was used. The reagents for the resolving gel and stacking gel were added to each other (**table 4**), and were left to polymerize for 30 min each. For electrophoresis, the running chamber from the Mini-Protean® Tetra Cell kit was used. To maintain a stable pH during electrophoresis, the running chamber was filled with running buffer (**table 3**). Then, after removing the combs, 10 µl Bio-rad marker was added into the first well of the gel. Finally, the samples were loaded into the other wells of the gel. The gel was run at 110 V using a Power Pac HC for 1.5 h, to separate the proteins according to size.

To blot the proteins onto a nitrocellulose membrane, the Mini-Trans-Blot® Cell kit was used. Therefore, the transfer cassette was assembled in the following way from bottom to top: black part of the cassette (-), sponge, chromatography paper, gel, nitrocellulose membrane, another piece of chromatography paper, a second sponge and finally the white part of the cassette (+), forming a “sandwich”. Then, the cassette was placed inside the transfer chamber, along with an ice tray and a magnetic stirrer, to avoid overheating. To ensure that the pH remains stable during the transfer, the chamber was filled with the transfer buffer, which was diluted with methanol and dH_2O. Finally, the transfer was run at 90 V for 1 h.

Table 2. Bradford assay

dH_2O	dH_2O	dH_2O	Sample 1	Sample 1	Sample 1
SC 0.05 µg/µl	SC 0.05 µg/µl	SC 0.05 µg/µl	Sample 2	Sample 2	Sample 2
SC 0.1 µg/µl	SC 0.1 µg/µl	SC 0.1 µg/µl	Sample 3	Sample 3	Sample 3
SC 0.2 µg/µl	SC 0.2 µg/µl	SC 0.2 µg/µl	Sample 4	Sample 4	Sample 4
SC 0.3 µg/µl	SC 0.3 µg/µl	SC 0.3 µg/µl	Sample 5	Sample 5	Sample 5
SC 0.4 µg/µl	SC 0.4 µg/µl	SC 0.4 µg/µl	Sample 6	Sample 6	Sample 6
SC 0.5 µg/µl	SC 0.5 µg/µl	SC 0.5 µg/µl	Sample 7	Sample 7	Sample 7
Lysis buffer	Lysis buffer	Lysis buffer	Sample 8	Sample 8	Sample 8

All samples, distilled H_2O (dH_2O), Lysis buffer, and standard curve solutions (SC) were pipetted in triplicates for more accurate measurement of the samples' protein concentrations.

3.2.7 Western Blot

3.2.7.1 The buffers

Table 3. The buffers used in western blots

Buffer:	Reagents:
10× running	30 g tris 144 g glycin 100 ml 10% SDS solution 1 l dH_2O
10× transfer	24.5 g tris 122 g glycin 1 l dH_2O

Washing	100 ml 10× PBS 1 ml tween 20 1 l dH_2O
5% blocking	50 g milk powder 1 l PBS
Stripping	62 ml tris (1 M, pH 6.8) 20 ml 10% SDS solution 1 l dH_2O

Reagents for 1 l of buffer.

Table 4. Reagents for 4 SDS gels

Reagents:	Resolving gel: 8%	10%	Stacking gel:
dH_2O	18.7 ml	15.9 ml	13.6 ml
30% (v/v) acrylamid	10.5 ml	13.3 ml	3.3 ml
1.5 M tris (pH 8.8)	10 ml	10 ml	2.5 ml
10% (v/v) SDS	200 µl	200 µl	200 µl
10% (m/v) APS	200 µl	200 µl	200 µl
TEMED	26 µl	26 µl	20 µl

3.2.7.2 Blocking, antibody incubation and protein visualization

After the proteins were blotted on the nitrocellulose membrane, the membrane was incubated with 5% milk buffer for 30 min to block the antibodies on the membrane. Then, the membrane was incubated with the primary antibody diluted 1:500 or 1:1000 (depending which antibody was used, **table 1**) with 5% milk buffer for either 1 h at room

temperature or overnight at 4 °C. After incubation with primary antibodies, the membrane was washed three times for 10 min using washing buffer. After washing, the membrane was incubated with secondary antibodies diluted 1:3000 with 5% milk buffer for 1 h at room temperature. Before visualization of the protein bands, the membrane was again rinsed three times for 10 min using washing buffer. To visualize the protein bands blotted on the nitrocellulose membrane, the membrane was incubated with SuperSignal® West Femto chemoluminescence substrate. After taking a picture of the marker, the protein bands were visualized by varying the exposure time until a representative image was taken.

3.2.7.3 Stripping the membrane

If, after visualizing protein bands, another protein of interest had a size as the protein investigated first, the membrane was stripped from its antibodies before it was incubated with the antibody for the second protein. Therefore, it was rinsed three times for 10 min, and then the membrane was incubated for 7 min at 52 °C with 50 ml stripping buffer and 347 µl 2-mercaptoethanol, to detach the antibodies from the nitrocellulose membrane. Once more, the membrane was washed 3 times with washing buffer for 10 min. Then, the proteins were blocked with 5% milk buffer, the membrane incubated with antibodies and the protein bands visualized as described in **3.2.7.2**

3.2.7.4 Processing the western blot data

After developing all proteins of interest and loading control, the density and size of the bands of the western blot were analysed using the ImageJ software.

Calculations: Normalized pixel density of the protein of interest/ Normalized pixel density of loading control

The result of this analysis is then exported to the GraphPad Prism Software to be even further analysed and plotted in a graph.

3.2.8 Migration assay

3.2.8.1 Seeding the fibroblasts

The fibroblasts were cultivated in a smaller 50 ml cell culture flask. The culture inserts were placed inside of the grid plates with a pair of tweezers. The insert is placed, so that

the centre part of the insert is aligned with one of the axes from the grid (**Fig. 10**). To prevent cells from migrating under the insert, it was important, that the insert was firmly placed onto the grid. The cells were passaged and counted as described in **3.1.2.1**. However, before counting, the cells were centrifuged at 13,249.6 × *g* for 8 min. From the total of 5 ml, 3 ml of the supernatant were discarded, leaving 2 ml, in which the cells were suspended. To count the cells, the cells were diluted 1:5 with trypan-blue were transferred into an Improved Neubauer counting chamber. The cells were counted manually, to improve the accuracy of the result.

Calculations: Total cells in reagent tube = *n* cells × 10,000 × 5 × 2 ml, where *n* is number of cells in 1 ml, determined by counting cells.

[c] (cells/ml) = Total cells/2 ml, where [c] is the concentration of cells in the flask

Volume/well (ml) = Cells needed per well × 1/[c]

9000 cells per well were loaded into the cell culture inserts, and were incubated until 70% confluence was reached

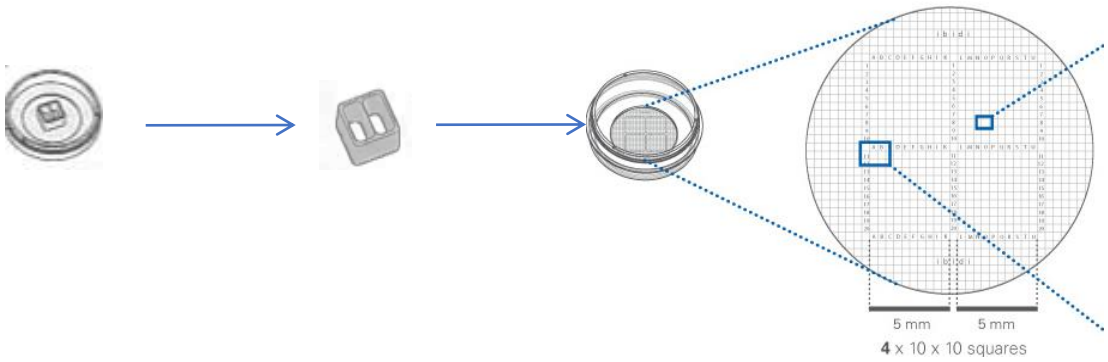

Figure 10. Positioning the cell culture insert. With a pair of tweezers, the insert is removed from the cell culture dish and placed onto the grid plate. Adapted from [92]

.

3.2.8.2 Transfection of the migration assay

The fibroblasts were transfected as described in **3.2.4**. Therefore, the transfection was executed as shown in **table 5** and **table 6**.

Table 5. Transfection for migration assay without stimulation

CTRL	OptiMEM™ only
SCR	OptiMEM™, Lipofectamine and scrambled microRNA
MIM34a	OptiMEM™, Lipofectamine and mimic miR-34a

CTRL: control, SCR: scrambled microRNA (miR), MIM34a: miR-34a mimic

Table 6. Transfection for migration assay without stimulation

CTRL	OptiMEM™ only
mock-PDGF	OptiMEM™ and Lipofectamine
mock+PDGF	OptiMEM™ and Lipofectamine
SCR	OptiMEM™, Lipofectamine and Scrambled microRNA
MIM34a	OptiMEM™, Lipofectamine and mimic miR-34a

CTRL: control, mock-PDGF: mock-platelet-derived growth factor, SCR: scrambled microRNA (miR), MIM34a: miR-34a mimic

3.2.8.3 Acquiring pictures and analysis

After the standard duration of the transfection, 24 h, the cell culture inserts were removed to create the gap between the fibroblasts. Then, pictures were taken with the Leica DMI 3000 B microscope and its camera at 0 h, 24 h and 48 h post transfection. If the fibroblasts were to be stimulated before taking pictures, it was done as described in **3.2.5**, with the difference, that the stimulant was left on the MLg fibroblasts until after taking all the pictures. The 24 h and 48 h pictures were compared to the 0 h pictures, so that only the cells that had migrated into the gap were counted. The cells were counted manually, and the data was inserted into the GraphPad Prism software for analysis.

4 Results

4.1 microRNA-34a, microRNA-34b and microRNA-34c expression levels are upregulated in mouse lung fibroblasts exposed to hyperoxia after 24 h and 48 h

In accordance to treatment of prematurely born infants, MLg fibroblasts, a cell-line, were exposed to 85% O_2 [31]. The levels of expression of miR-34a, miR-34b and miR-34c were determined by real-time qPCR and compared to a control group, which was exposed to only 21% O_2. It was revealed that the delta cycle threshold (ΔC_T) of miR-34a, miR-34b and miR-34c in MLg fibroblasts exposed to 85% O_2 was significantly higher than the ΔC_T of miR-34a, miR-34b and miR-34c in MLg fibroblasts in the control group, after 24 h exposure to 85% O_2 as well as 48 h exposure (**Fig. 11**). Also, it was observed, that MLg fibroblasts that dwelled in 85% O_2 for 48 h exhibited a stronger increase in miR-34a, miR-34b and miR-34c expression levels, than the MLg fibroblasts that were left at 85% O_2 for only 24 h. Finally, it was found that the ΔC_T of miR-34a in MLg fibroblasts after 48 h exposure to 85% O_2 was at a higher value than the ΔC_T of miR-34b and the ΔC_T of miR-34c after 48 h in 85% O_2 (**Fig. 11)**. In conclusion, it can be stated, that miR-34a, miR-34b and miR-34c expression levels were brought up by exposure to 85% O_2 for 24 h, and even more so for 48 h, and that miR-34a had the highest levels of expression after 48 h exposure to 85% O_2, compared to the expression levels of miR-34b and miR-34c. The fact that miR-34a expression was higher after exposure to high levels of oxygen than miR-34b and miR-34c, justifies that miR-34a was chosen for further examination, rather than miR-34b or miR-34c.

4.2 Platelet-derived growth factor receptor α and platelet-derived growth factor receptor β are downregulated in mouse lung fibroblasts after 24 h and 48 h exposure to hyperoxia

It has been reported that PDGFRα and PDGFRβ are targets of miR-34a [93]. Additionally, playing an important role in late lung development [83] PDGFRα and additionally PDGFRβ were selected to be examined, in order to investigate the role of

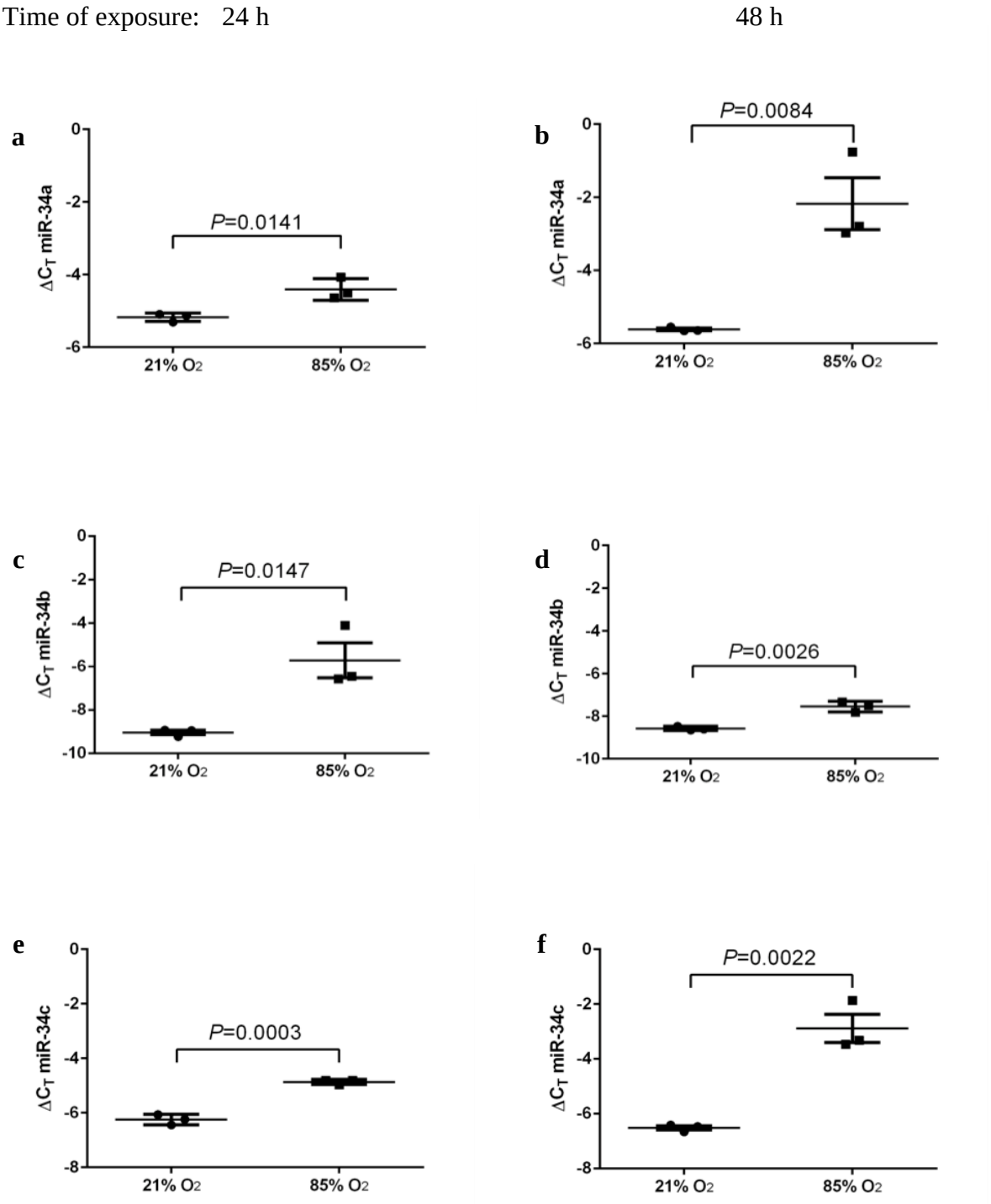

Figure 11. The miR-34 family is upregulated in mouse lung fibroblasts under hyperoxic conditions. Levels of microRNA (miR)-34a (a-b), miR-34b (c-d), miR-34c (e-f) expression are increased in Mouse Lung (MLg) fibroblasts exposed to 85% O_2 compared to 21% O_2 for 24 h (**a, c, e**) and 48 h (**b, d, f**). Results were obtained by real-time qPCR, where *n*=3. Values are means ± SEM. An unpaired Students *t*-test was used to determine *P*-values.

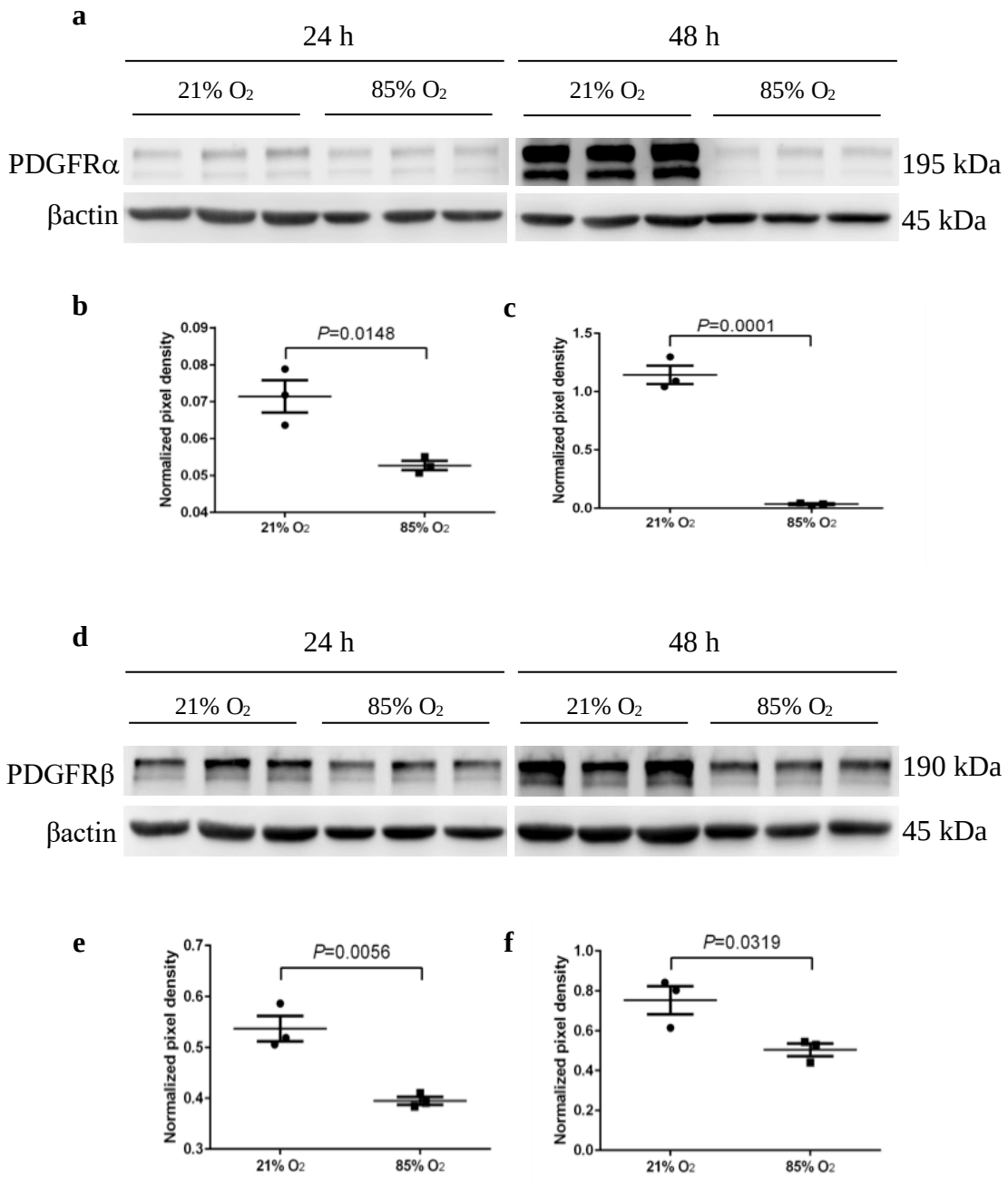

Figure 12. PDGFR α and β levels are reduced in mouse lung fibroblasts under hyperoxic conditions. Platelet-derived growth factor receptor α (a-c) and platelet-derived growth factor receptor β (d-f) are downregulated in mouse lung fibroblasts after exposure to 85% O_2 for 24 h (b, e) and 48 h (c, f). Protein expression was assessed by western blot, where *n*=3 and βactin was loading control. Values are means ± SEM. An unpaired Students *t*-test was used to determine *P*-values.

miR-34a on fibroblasts migration. Seeing as how expression levels of miR-34a were elevated in MLg fibroblasts after exposure to 85% O_2, MLg fibroblasts were incubated at

21% O_2 and 85% O_2 for 24 h and 48 h, to be examined whether levels of PDGFRα and PDGFRβ were affected by high levels of oxygen accordingly. Western blots showed that the amount of PDGFRα and PDGFRβ in MLg fibroblasts after 24 h and 48 h long exposure to 85% O_2, was significantly lower than equally long exposure to 21% O_2 (**Fig. 12**). It was also revealed that after 48 h of exposure to 85% O_2 PDGFRα was more drastically downregulated than after only 24 h of the same high-level oxygen treatment (**Fig. 12**). PDGFRβ levels, even though clearly downregulated after both 24 h and 48 h of exposure to high levels of oxygen did not react as strongly to doubling the exposure time to high levels of oxygen, as PDGFRα (**Fig. 12**)**.** Therefore, high levels of oxygen downregulated both PDGFRα and PDGFRβ protein levels in MLg fibroblasts, maintained under hyperoxic conditions for 24 h and 48 h.

4.3 Platelet-derived growth factor receptor α and platelet-derived growth factor receptor β are downregulated in mouse lung fibroblasts after microRNA-34a over expression

Considering that 85% O_2 significantly upregulated miR-34a and downregulated PDGFRα and PDGFRβ in MLg fibroblasts, the next step was to explore whether miR-34a downregulates PDGFRα and PDGFRβ levels in MLg fibroblasts. For that, MLg fibroblasts were transfected with either a miR-34a mimic or scrambled miR, which was the control group. The western blots showed, that in the miR-34a transfected MLg fibroblasts, levels of PDGFRα and PDGFRβ were significantly lower than in the MLg fibroblasts, which were transfected with scrambled miR (**Fig 13**). To conclude, miR-34a had a downregulating effect on PDGFRα and PDGFRβ protein levels in MLg fibroblasts after 24 h of transfection. These results suggest miR-34a as part of the mechanism that drove the downregulation of PDGFRα and PDGFRβ protein levels in MLg fibroblasts under hyperoxic conditions.

4.4 No significant change in phosphorylation of AKT and ERK in mouse lung fibroblasts after microRNA-34a over expression

AKT and ERK, downstream signalling molecules of PDGFRα and PDGFRβ [67, 68], were investigated, because AKT and ERK were shown to promote fibroblast migration

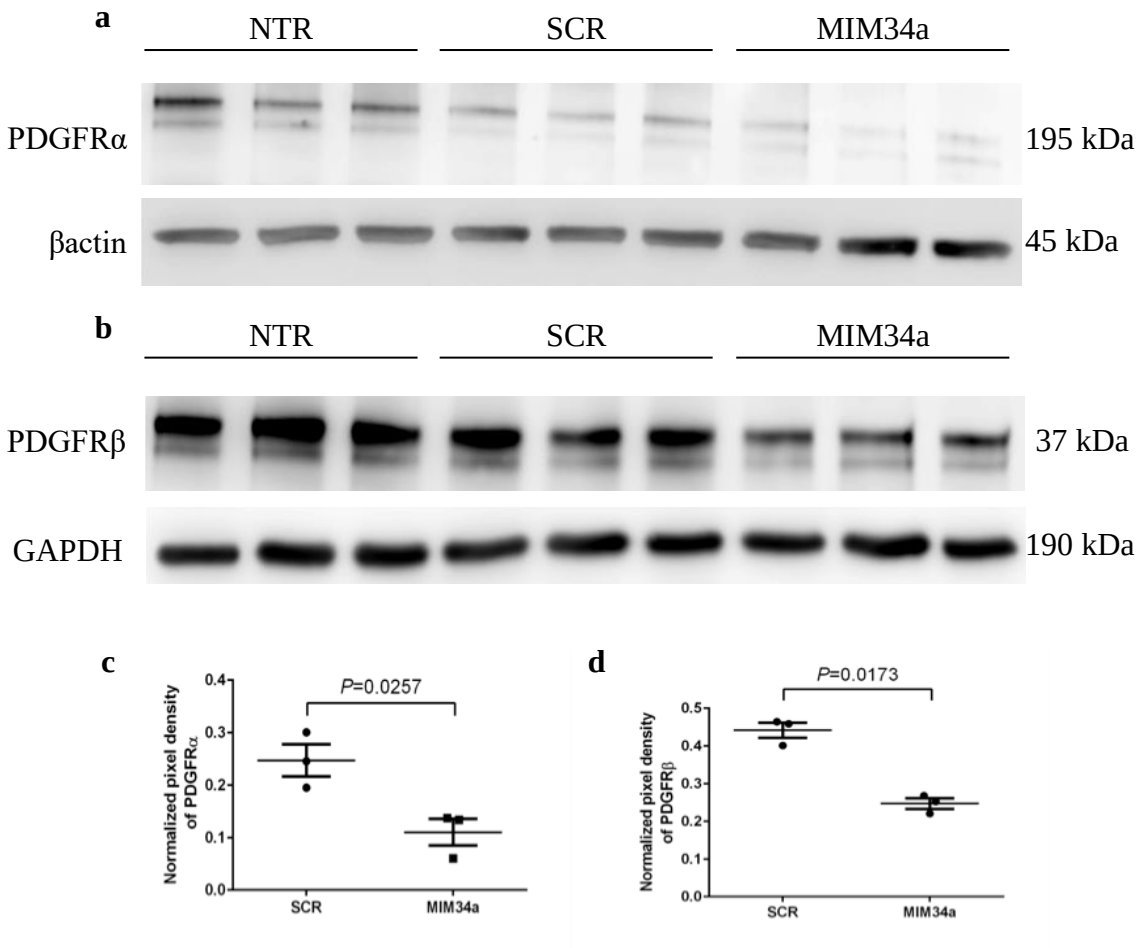

Figure 13. PDGFR α and β are downregulated by over expressing miR-34a in mouse lung fibroblasts. Over expression of microRNA-34a in Mouse Lung fibroblasts downregulates Platelet-derived growth factor receptor α (a, c) and Platelet-derived growth factor receptor β (b, d). The Mouse Lung (MLg) fibroblasts were transfected with 80 nM scrambled (SCR) microRNA and microRNA-34a mimic (MIM34a) for 24 h, or not transfected (NTR), where *n*=3. Protein expression was assessed by western blot, where βactin and Glyceraldehyde 3-phosphate dehydrogenase (GAPDH) were loading control. Values are means ± SEM. An unpaired Students *t*-test was used to determine *P*-values.

and proliferation [94]. AKT gene upregulation was also proven to preserve alveolar structure in a new born rat model of hyperoxia induced BPD [95]. With these pre-existing implications that AKT and ERK play important roles in lung alveolarization, these downstream signalling molecules seemed like the logical choice to further investigate the impact of miR-34a on the PDGF receptors and on fibroblast migration. Measuring the

activation of AKT and ERK was an attempt to further specify the connection between miR-34a expression and fibroblast migration by examining the effect of miR-34a on the downstream signalling on two of its targets, PDGFR α and β.

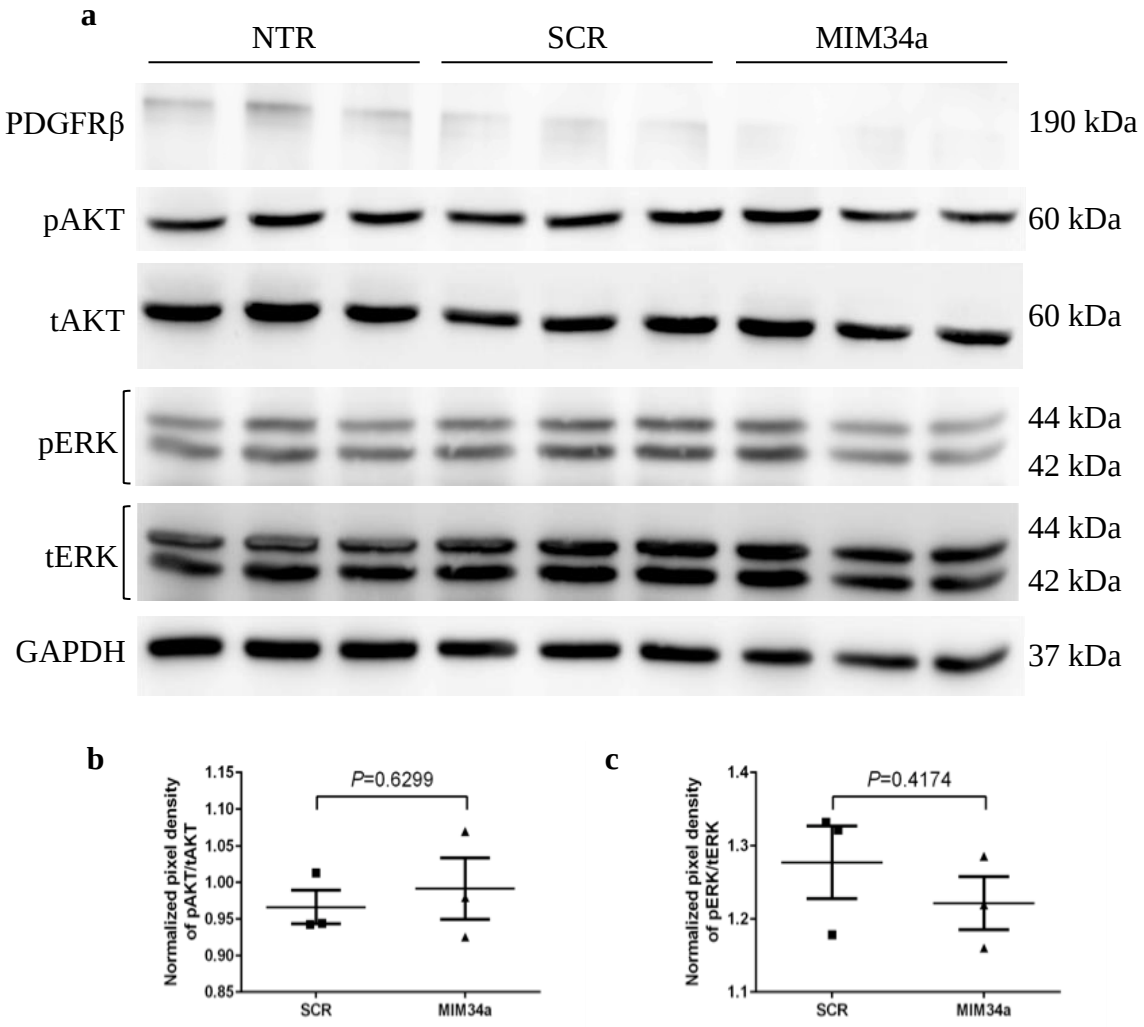

Figure 31. AKT and ERK phosphorylation remains unaffected after miRNA-34a over expression in mouse lung fibroblasts. AKT (a-b), ERK (a, c). Transfection of mouse lung (MLg) fibroblasts with 80 nM scrambled (SCR) miroRNA and microRNA-34a mimic (MIM34a) for 24 h, and not transfected (NTR), where *n*=3. Protein expression was assessed by western blot, where Glyceraldehyde 3-phosphate dehydrogenase (GAPDH) was loading control and platelet-derived growth factor receptor (PDGFRβ) was transfection control. Values are means ± SEM. An unpaired Students *t*-test was used to determine *P*-values. Primary antibodies against PDGFRβ, phosphorylated AKT (pAKT), total AKT (tAKT), phosphorylated ERK (pERK), total ERK (tERK) and GAPDH were used.

Low levels of activated downstream signalling molecules are a sign for lesser receptor activation, therefore lower levels of activated AKT and ERK would illustrate downregulation of PDGF receptor expression. So, the ratio of phosphorylated AKT and phosphorylated ERK to the total amount of AKT and ERK was determined in miR-34a transfected MLg fibroblasts by western blot. As transfection control, the MLg fibroblasts exhibited downregulation of PDGFRβ protein levels in miR-34a transfected MLg fibroblasts (**Fig. 14a**). The western blot however shows no significant difference between the relation of activated AKT and total AKT in miR-34a mimic transfected MLg fibroblasts (**Fig. 14a** and **b**). When testing for ERK, similar results showed (**Fig. 14a** and **c**). Therefore, it can be concluded, that transfecting MLg fibroblasts with miR-34a mimic has a downsizing effect on PDGFRα and PDGFRβ expression, but no effect on its rate of activation of the PDGF receptor pathway in form of AKT or ERK phosphorylation.

4.5 AKT and ERK pathway activation is reduced in mouse lung fibroblasts after microRNA-34a over expression and stimulation of platelet-derived growth factor receptor α with its ligand PDGFA

It has been reported that PDGFA is a specific ligand of PDGFRα [79]. Since the AKT and ERK signalling pathways of the PDGF receptors failed to activate significantly after transfecting MLg fibroblasts with miR-34a in an unstimulated situation, the consequent measure was to stimulate PDGFRα with its ligand after transfection with miR-34a mimic to investigate, whether the activation of PDGFRα is affected by miR-34a in MLg fibroblasts. Therefore, MLg fibroblasts were treated with PDGFA to stimulate PDGFRα, after over expressing miR-34a in the fibroblasts by transfection. The western blots from these fibroblasts showed downregulation of PDGFRα in miR-34a transfected MLg fibroblasts, showing that the transfection of the MLg fibroblasts was successful (**Fig. 15a**). As stimulation control, the western blots also showed a stronger activation of AKT (**Fig. 15a** and **d**) and ERK (**Fig. 15a** and **e)** signalling pathways in fibroblasts stimulated with PDGFA, than in the fibroblasts without stimulation. And finally, the MLg fibroblasts exhibit diminished activation of AKT (**Fig. 15a** and **b**) and ERK (**Fig. 15a** and **c**) signalling pathways if transfected with miR-34a and treated with PDGFA.

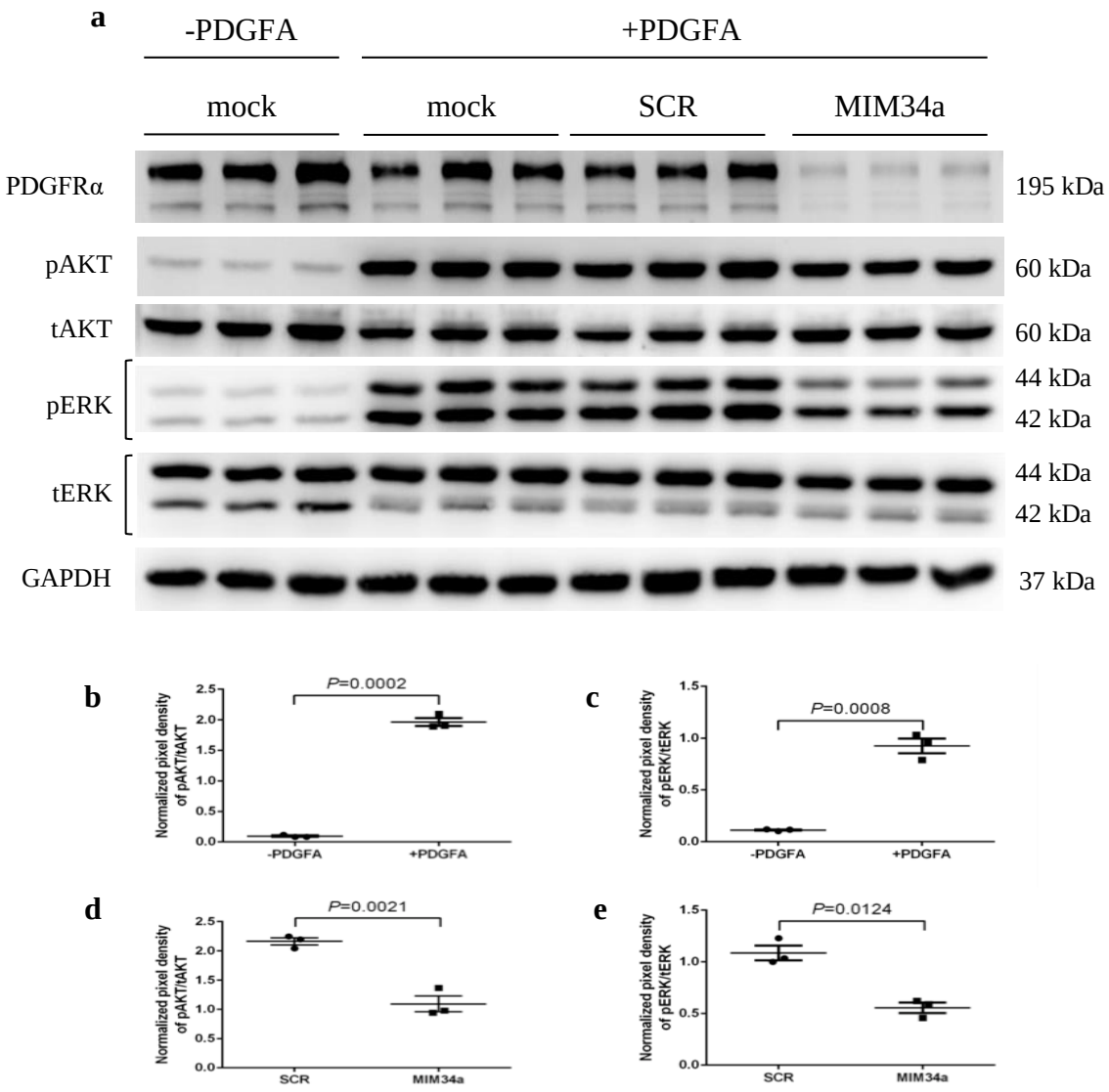

Figure 15. AKT and ERK phosphorylation is downregulated in platelet-derived growth factor A stimulated mouse lung fibroblasts after miRNA-34a over expression. AKT (a, d) and ERK (a, e). Mouse lung (MLg) fibroblasts were transfected with 80 nM scrambled (SCR) microRNA and 80 nM microRNA-34a mimic (MIM34a) for 24 h, and stimulated with platelet-derived growth factor (PDGF) A, where *n*=3. Mock samples were not transfected. Protein expression was assessed by western blot, where Glyceraldehyde 3-phosphate dehydrogenase (GAPDH) was loading control and PDGF receptor (PDGFR)α was transfection control (**a**). AKT (**a-b**) and ERK (**a, c**) phosphorylation is amplified in PDGFA treated MLg fibroblasts (stimulation control). Values are means ± SEM. An unpaired Students *t*-test was used to determine *P*-values. Primary Antibodies of phosphorylated AKT (pAKT), total AKT (tAKT), phosphorylated ERK (pERK), total ERK (tERK), PDGFRα and GAPDH were used.

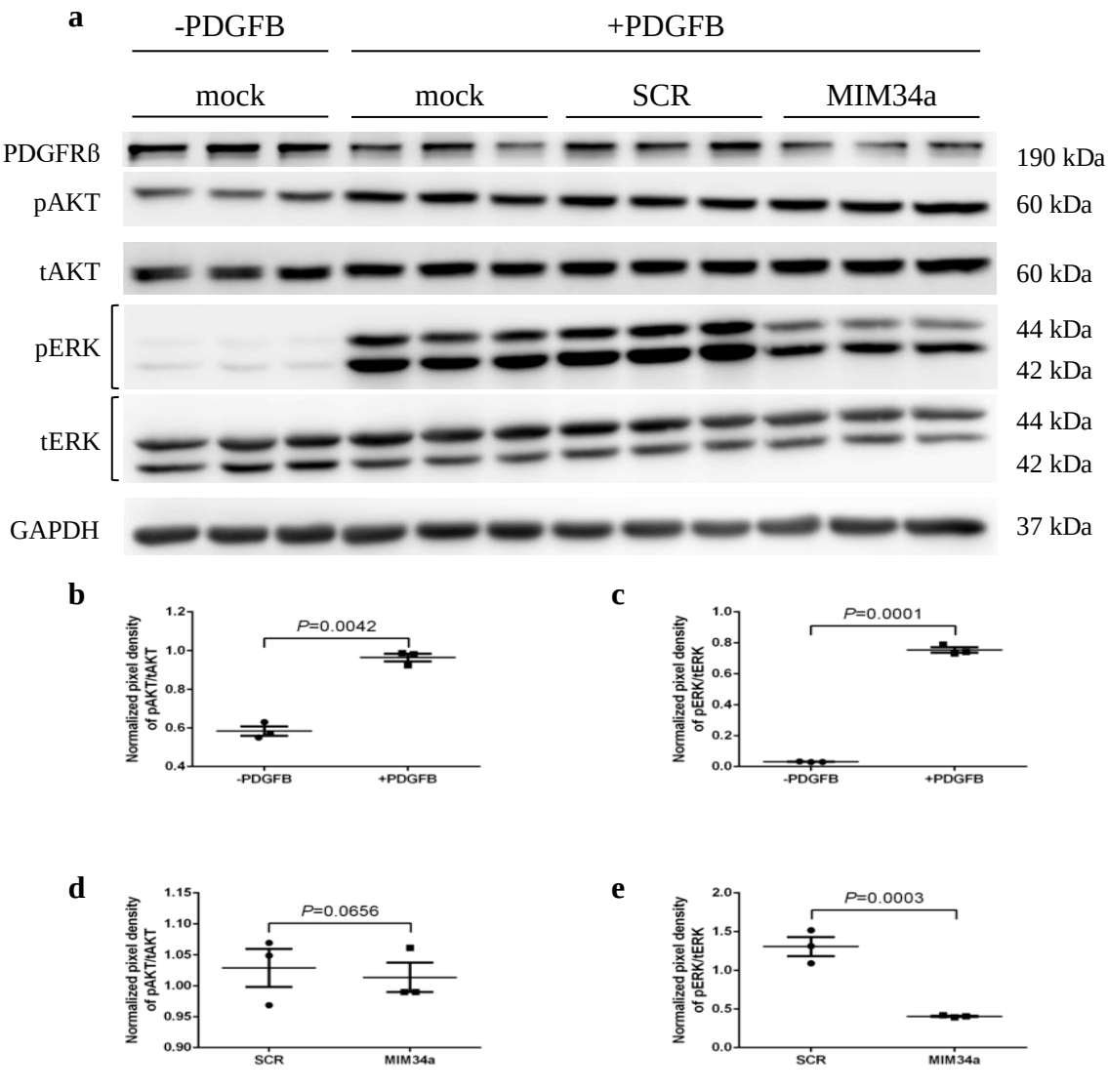

Figure 16. AKT activation remains unaffected and ERK activation is inhibited in platelet-derived growth factor B treated mouse lung fibroblasts after miRNA-34a over expression. AKT (a-d) and ERK (a, e). Mouse lung (MLg) fibroblasts were transfected with 80 nM scrambled (SCR) microRNA and 80 nM microRNA-34a mimic (MIM34a) for 24 h, and stimulated with platelet-derived growth factor (PDGF) A, where *n*=3. Mock samples were not transfected. Protein expression was assessed by western blot, where Glyceraldehyde 3-phosphate dehydrogenase (GAPDH) was loading control and PDGF receptor (PDGFR) β was transfection control. AKT (**a-b**) and ERK (**a, c**) phosphorylation is amplified in PDGFB stimulated MLg fibroblasts (Stimulation control). Values are means ± SEM. An unpaired Students *t*-test was used to determine *P*-values. Primary Antibodies of phosphorylated AKT (pAKT), total AKT (tAKT), phosphorylated ERK (pERK), total ERK (tERK), PDGFRβ and GAPDH were used.

To conclude, miR-34a over expression reduces AKT and ERK activation in MLg fibroblasts that were stimulated with PDGFA. Considering PDGFRα was stimulated with its specific ligand [79], it can be concluded, that the reduction of AKT and ERK activation is caused by downregulation of PDGFRα by miR-34a.

4.6 Treating mouse lung fibroblasts with PDGFB after transfection with microRNA-34a shows reduction of ERK activation and no change of AKT activation

Previous studies show that PDGFB is a ligand to both of PDGFRα and PDGFRβ [79]. To further examine whether the activation of PDGFRα and PDGFRβ is affected by miR-34a over expression, MLg fibroblasts were treated with PDGFB after transfecting the fibroblasts with miR-34a mimic. The results from these western blots showed downregulation of PDGFRβ in miR-34a transfected MLg fibroblasts, demonstrating that transfection of the MLg fibroblasts was successful (**Fig. 16a**). As stimulation control, the western blots also showed a stronger activation of AKT (**Fig. 16a** and **d**) and ERK (**Fig. 16a** and **e)** signalling pathways in fibroblasts stimulated with PDGFB, than in the fibroblasts without stimulation, demonstrating successful stimulation of PDGFRβ. Differently from stimulation with PDGFA, stimulation of the MLg fibroblasts with PDGFB after over expressing miR-34a, demonstrated that the AKT signalling pathway was not significantly affected (**Fig. 16a** and **b**). However, similarly when stimulating with PDGFA, PDGFB stimulation of MLg fibroblasts revealed reduced activation of ERK (**Fig. 16a** and **c**). This therefore signifies that PDGFB stimulation of miR-34a transfected MLg fibroblasts shows reduced activation of the ERK signalling pathway and not the AKT signalling pathway. Keeping in mind that PDGFB binds to both PDGFRα and PDGFRβ [79], it can be assumed that the reduced activation of ERK is caused by miR-34a induced downregulation of the PDGF receptors.

4.7 Treating mouse lung fibroblasts with PDGFD after transfection with microRNA-34a shows reduction of ERK activation and no change of AKT activation

It has been reported that PDGFD binds to PDGFRβ specifically [80], although research also suggests it is also a ligand to the PDGFRα and PDGFRβ heterodimer [96]. Aiming at establishing a connection between miR-34a and PDGFRβ, PDGFRβ was stimulated with its ligand PDGFD [80] after transfecting MLg fibroblasts with miR-34a mimic. The results showed downregulation of PDGFRβ in miR-34a transfected MLg fibroblasts, showing that transfection of the MLg fibroblasts was successful (**Fig. 17a**). Contrary to the stimulation controls obtained when stimulating with PDGFA and PDGFB, the rate of activation of both AKT and ERK signalling pathways was reduced in PDGFD treated MLg fibroblasts, compared to non-stimulated fibroblasts. (**Fig. 17a**, **d** and **e**) However, similarly to stimulation with PDGFB, stimulation of the MLg fibroblasts with PDGFD after transfection with miR-34a mimic, demonstrated that the rate of activation of the ERK signalling pathway was significantly reduced in miR-34a over expressing MLg fibroblasts **(Fig. 17a** and **c)**. Also, similarly to stimulation with PDGFB, the results show that the activation of the AKT signalling pathway was not affected in fibroblasts over expressing miR-34a (**Fig. 17a** and **b**). In conclusion, PDGFD treatment of miR-34a transfected MLg fibroblasts shows reduction of activation of the ERK signalling pathway and not the AKT signalling pathway.

4.8 Over expression of microRNA-34a inhibits migration in mouse lung fibroblasts

Since migration is such a dominant feature in late lung development [11], a migration assay was performed, to examine the effects of miR-34a at a functional level. The results of the migration assay show that migration is not yet reduced after 24 h in miR-34a transfected cells (**Fig. 18a**, **b** and **d**). However, migration is reduced in mir-34a over expressing cells after 48h. The control samples, cells without any transfection, had the most cells after 24 h and after 48 h post transfection and had formed a confluent layer of cells, which was too dense to quantify in numbers (**Fig. 18a** and **d**). Thus, proving that migration was

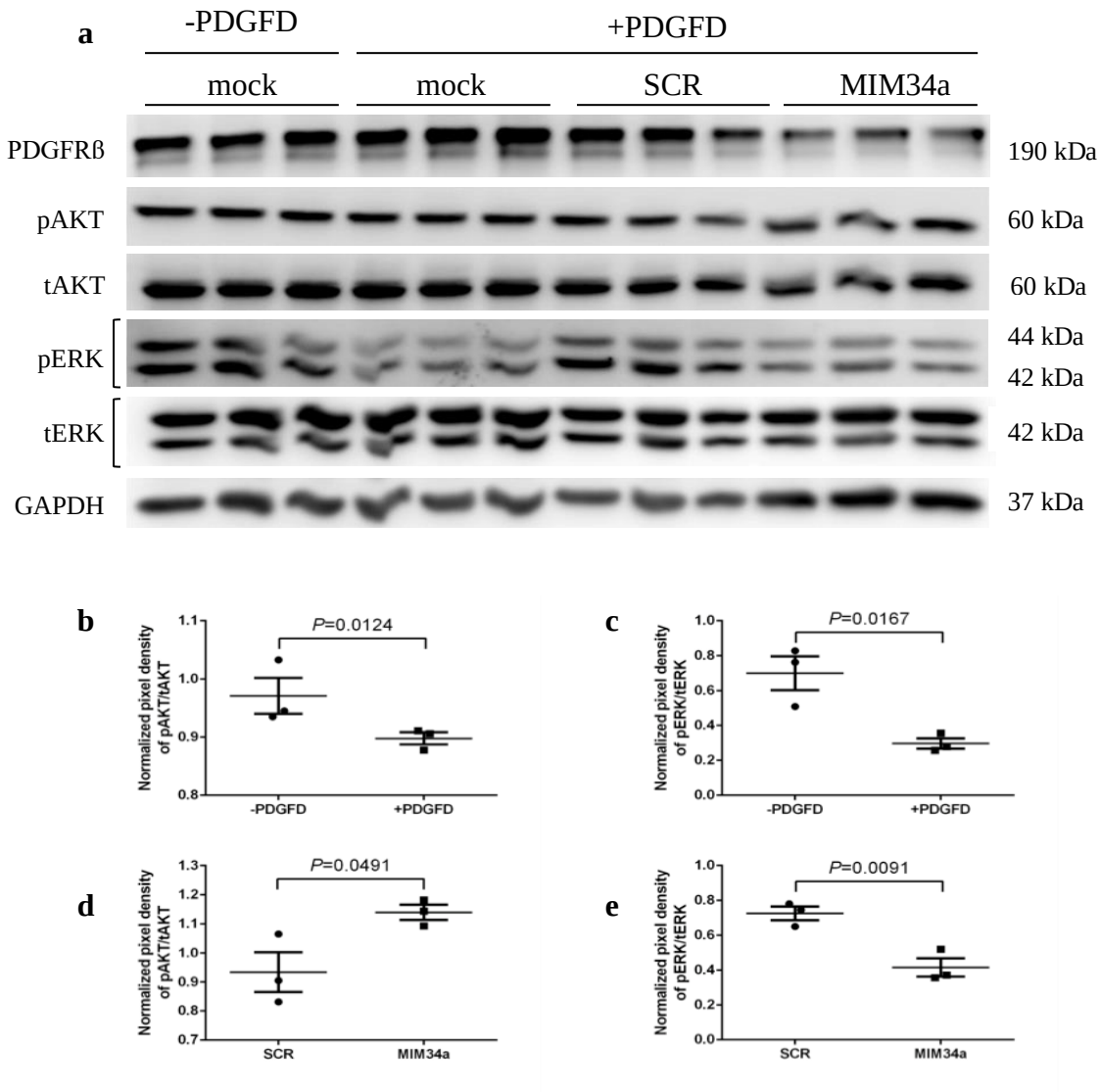

Figure 17. AKT activation remains unaffected and ERK activation is inhibited in platelet-derived growth factor D treated mouse lung fibroblasts after miRNA-34a over expression. AKT (a-d) and ERK (a, e). Mouse lung (MLg) fibroblasts were transfected with 80 nM scrambled (SCR) microRNA and 80 nM microRNA-34a mimic (MIM34a) for 24 h, and stimulated with platelet-derived growth factor (PDGF) A, where *n*=3. Mock samples were not transfected. Protein expression was assessed by western blot, where Glyceraldehyde 3-phosphate dehydrogenase (GAPDH) was loading control and PDGF receptor (PDGFR) β was transfection control. AKT (**a-b**) and ERK (**a, c**) phosphorylation is decreased in PDGFD stimulated MLg fibroblasts (Stimulation control). Values are means ± SEM. An unpaired Students *t*-test was used to determine *P*-values. Primary Antibodies of phosphorylated AKT (pAKT), total AKT (tAKT), phosphorylated ERK (pERK), total ERK (tERK), PDGFRβ and GAPDH were used.

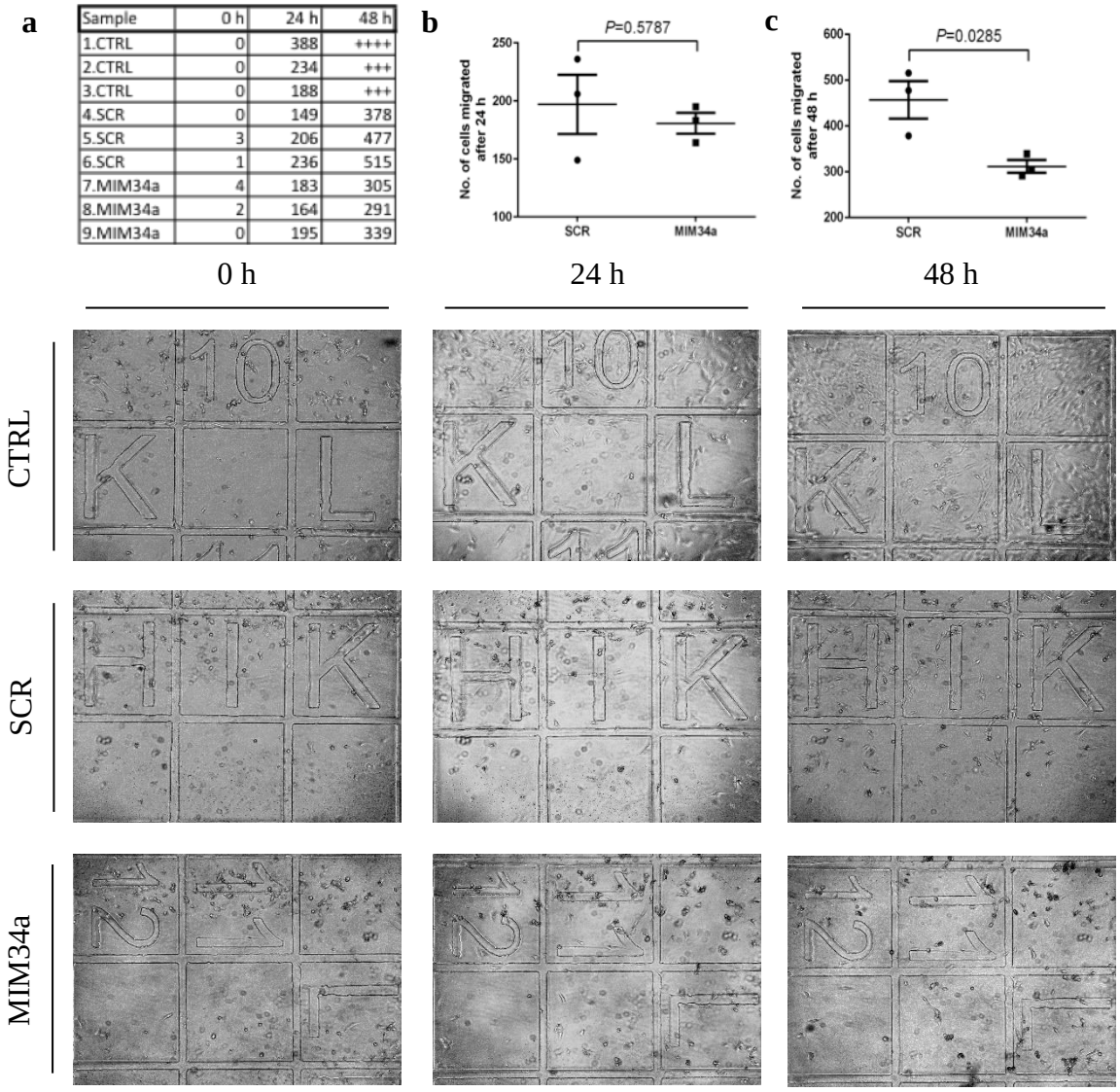

Sample	0 h	24 h	48 h
1.CTRL	0	388	++++
2.CTRL	0	234	+++
3.CTRL	0	188	+++
4.SCR	0	149	378
5.SCR	3	206	477
6.SCR	1	236	515
7.MIM34a	4	183	305
8.MIM34a	2	164	291
9.MIM34a	0	195	339

Figure 18. MiR-34a reduces fibroblast migration. Over expression of microRNA-34a reduces migration in fibroblasts after 48 h (a, c). Migration is not reduced after 24 h (a-b). Transfection of the mouse lung (MLg) fibroblasts with 80nM scrambled microRNA (SCR) an and miR-34a mimic (MIM34a) for 24 h, where *n*=3. Control samples (CTRL) were not transfected. Migration was assessed by cell assay. Representative pictures are shown from the samples control (CTRL), SCR and MIM34a taken after 0 h, 24 h and 48 h after transfection. (d) Values are means ± SEM. An unpaired Students *t*-test was used to determine *P*-values. +++++ = 95% of gap area covered by fibroblasts, ++++ = 90% of gap area covered by fibroblasts, +++= 85% of gap area covered by fibroblasts.

indeed inhibited by miR-34a mimic transfection and not by an error in method. In conclusion, it can be said, that miR-34a over expression reduces migration in MLg fibroblasts after 48 h.

4.9 Over expressing microRNA-34a before stimulating with platelet-derived growth factor A inhibits migration in mouse lung fibroblasts

PDGFRα and its specific ligand PDGFA [79] are key players in fibroblast migration [83]. To establish whether miR-34a inhibits fibroblast migration through PDGFRα, the MLg fibroblasts were treated with the specific ligand for PDGFRα, PDGFA, [79] after transfecting the fibroblasts with miR-34a mimic in a migration assay. The results from the migration assay showed that the control samples had migrated to close the gap with a confluent layer after 48 h (**Fig. 19a, Fig 22**). The stimulation control also revealed that PDGFA treated fibroblasts had a higher rate of migration than the fibroblasts without treatment with PDGFA after 24 h (**Fig. 19a, d** and **Fig 22**) and 48 h (**Fig. 19a, e** and **Fig 22**). Finally, the migration assay showed, that if treated with PDGFA, MLg fibroblasts which were transfected with miR-34a mimic were migrating significantly less than fibroblasts that were transfected with scrambled miR after 24 h (**Fig. 19a, b** and **Fig 22**) and 48 h post transfection (**Fig. 19a, c** and **Fig 22**) Therefore, it can be said, that the reduced rate of migration of miR-34a over expressing MLg fibroblasts is caused by miR-34a mimic induced downregulation of PDGFRα. This also means that stimulation of miR-34a transfected MLg fibroblasts with PDGFA, showed results of inhibited migration already after 24 h post transfection, compared to the non-stimulated migration assay, in which the effect of miR-34a was only observed after 48 h. The control samples demonstrated that migration was indeed inhibited by miR-34a mimic transfection and not by an error in method (**Fig. 19a** and **Fig 22**).

4.10 Transfection with microRNA 34a before stimulating with platelet-derived growth factor B reduces migration of mouse lung fibroblasts

PDGFB binds to both PDGFRα and PDGFRβ [79] and is therefore also a crucial element in fibroblast migration [83]. To investigate whether miR-34a inhibits fibroblast migration by affecting PDGFRα and PDGFRβ, the MLg fibroblasts were treated with PDGFB, after over expressing miR-34a in the MLg fibroblasts in a migration assay. The

a

Stimulation	Sample	0 h	24 h	48 h
no stimulation	1.CTRL	0	614	+++++
no stimulation	2.CTRL	0	611	++++
no stimulation	3.CTRL	0	673	++++
no stimulation	4.mock	0	449	2135
no stimulation	5.mock	0	466	2235
no stimulation	6.mock	0	606	2547
PDGFA	7.mock	0	854	3706
PDGFA	8.mock	0	791	3258
PDGFA	9.mock	0	812	3567
PDGFA	10.SCR	0	482	2087
PDGFA	11.SCR	0	573	2538
PDGFA	12.SCR	0	526	2396
PDGFA	13.MIM34a	0	356	1051
PDGFA	14.MIM34a	0	330	943
PDGFA	15.MIM34a	0	341	1173

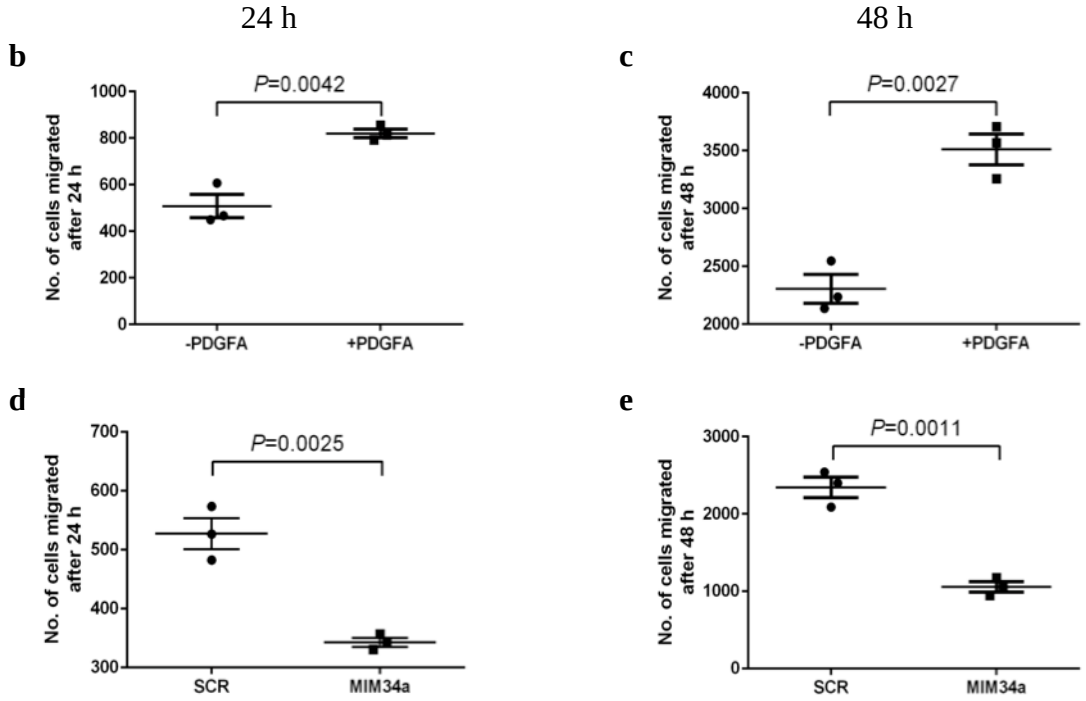

Figure 19. Over expression of miRNA-34a inhibits migration in PDGF A treated fibroblasts after 24 h and after 48 h (analysis). 24 h (a, d) and 48 h (a, e). Mouse lung (MLg) fibroblasts were transfected with 80nM scrambled microRNA (SCR) and microRNA-34a mimic (MIM34a) for 24 h, and stimulated with platelet-derived growth factor (PDGF) A, where *n*=3. Control (CTRL) and mock samples were not transfected. Migration was assessed by cell assay, where mock was stimulation control (**a-c**). Values are means ± SEM. An unpaired Students *t*-test was used to determine *P*-values. +++++ = 95% of gap area covered by fibroblasts, ++++ = 90% of gap area covered by fibroblasts, +++= 85% of gap area covered by fibroblasts. Representative images shown in Appendix (**Fig. 21**).

a

stimulation	Sample	0 h	24 h	48 h
no stimulation	1.CTRL	0	260	++++
no stimulation	2.CTRL	0	190	+++
no stimulation	3.CTRL	0	239	+++
no stimulation	4.mock	0	217	639
no stimulation	5.mock	0	169	474
no stimulation	6.mock	0	196	615
PDGFB	7.mock	0	331	909
PDGFB	8.mock	0	291	891
PDGFB	9.mock	0	259	783
PDGFB	10.SCR	0	255	676
PDGFB	11.SCR	0	234	632
PDGFB	12.SCR	0	221	479
PDGFB	13.MIM34a	0	91	293
PDGFB	14.MIM34a	0	58	140
PDGFB	15.MIM34a	0	83	101

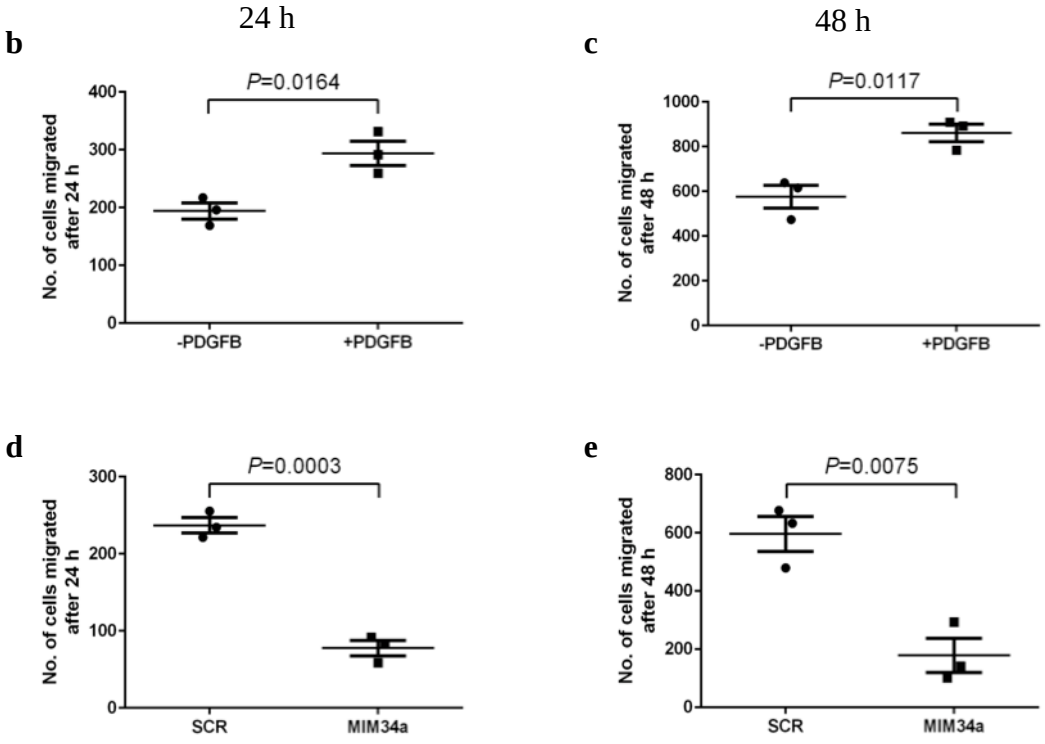

Figure 20. Over expression of miRNA-34a inhibits migration in PDGFB treated fibroblasts after 24 h and after 48 h (analysis). 24 h (a, d) and 48 (a, e). Mouse lung (MLg) fibroblasts were transfected with 80nM scrambled microRNA (SCR) and microRNA-34a mimic (MIM34a) for 24 h, and stimulated with platelet-derived growth factor (PDGF) B, where *n*=3. Control (CTRL) and mock samples were not transfected. Migration was assessed by cell assay, where mock was stimulation control (a-c). Values are means ± SEM. An unpaired Students *t*-test was used to determine *P*-values. +++++ = 95% of gap area covered by fibroblasts, ++++ = 90% of gap area covered by fibroblasts, +++= 85% of gap area covered by fibroblasts. Representative images shown in Appendix (**Fig. 22**)

control samples had migrated to close the gap with a confluent layer after 48 h (**Fig. 20a** and **Fig 23**). The stimulation control revealed, that treatment with PDGFB led to a higher rate of migration in MLg fibroblasts, than in fibroblasts without treatment with PDGFB after 24 h (**Fig. 20a, d** and **Fig 23**) and 48 h (**Fig. 20a, e** and **Fig 23**). The results showed, that if treated with PDGFB, MLg fibroblasts that were over expressing miR-34a were migrating significantly less than fibroblasts that were not over expressing miR-34a after 24 h (**Fig. 20a, b** and **Fig 23**) and 48 h post transfection (**Fig. 20a, c** and **Fig 23**). Hence, the reduced rate of migration of miR-34a over expressing MLg fibroblasts is a result of miR-34a mimic induced downregulation of PDGFRα and PDGFRβ. The control samples showcase that migration was indeed inhibited by miR-34a over expression and not by an error in method (**Fig. 20a** and **Fig 23**).

4.11 Transfection with microRNA 34a before stimulating with platelet-derived growth factor D reduces migration of mouse lung fibroblasts

PDGFD binds to PDGFRβ [80] and is therefore also an important element in fibroblast migration [83] To examine whether miR-34a decreases fibroblast migration by influencing PDGFRβ, the MLg fibroblasts were treated with PDGFD, after over expressing miR-34a in the MLg fibroblasts in a migration assay. The control samples had closed the gap by migrating with a confluent layer after 48 h (**Fig. 21a** and **Fig. 24**). Unexpectedly, the stimulation control shows, that stimulating the fibroblasts with PDGFD, caused the MLg fibroblasts to migrate less than PDGFD treated fibroblasts after 24 h (**Fig. 21a, d** and **Fig. 24**) and 48 h (**Fig. 21a, e** and **Fig. 24**), which contradicts the results from the other migration assays, although it is in concurrence with the results from **4.7.** At last, the migration assay showed, that if treated with PDGFD, MLg fibroblasts that were transfected with miR-34a mimic were migrating significantly less than fibroblasts that were not over expressing miR-34a after 24 h (**Fig. 21a, b** and **Fig. 24**) and 48 h post transfection (**Fig. 21a, c** and **Fig. 24**). In conclusion, even though over expression of miR-34a in MLg fibroblasts before treatment with PDGFD did have a decreasing effect on fibroblast migration, stimulating the fibroblasts with PDGFD did not improve migration, opposed to treatment with PDGFB and PDGFA, but is consistent with results from the PDGFD stimulated western blot. The control samples

demonstrated that migration was indeed inhibited by miR-34a mimic transfection and not by an error in method (**Fig. 21a** and **Fig. 24**).

a

Stimulation	Sample	0 h	24 h	48 h
no stimulation	1.CTRL	0	374	+++
no stimulation	2.CTRL	0	452	+++
no stimulation	3.CTRL	0	439	+++
no stimulation	4.mock	0	366	921
no stimulation	5.mock	0	271	899
no stimulation	6.mock	0	306	1021
PDGFD	7.mock	0	178	567
PDGFD	8.mock	0	165	626
PDGFD	9.mock	0	221	741
PDGFD	10.SCR	0	156	501
PDGFD	11.SCR	0	197	634
PDGFD	12.SCR	0	148	437
PDGFD	13.MIM34a	0	98	235
PDGFD	14.MIM34a	0	102	342
PDGFD	15.MIM34a	0	99	294

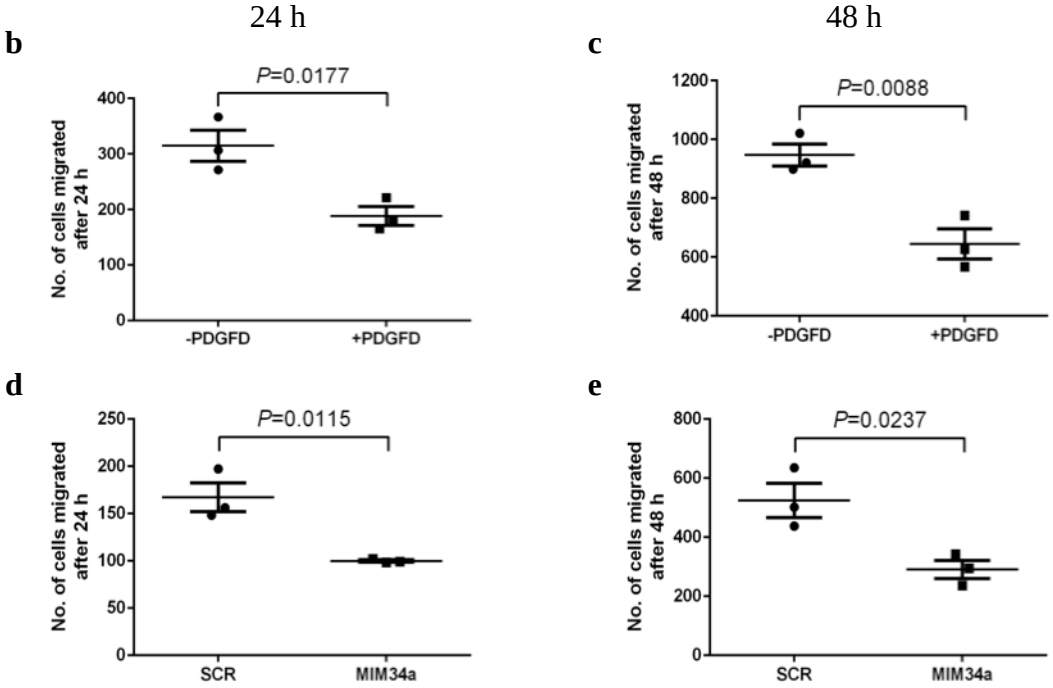

Figure 21. Over expression of miRNA-34a inhibits migration in PDGFD treated fibroblasts after 24 h and after 48 h (analysis). 24 h (a, d) and 48 h (a, e) Mouse lung (MLg) fibroblasts were transfected with 80nM scrambled microRNA (SCR) and microRNA-34a mimic (MIM34a) for 24 h, and stimulated with platelet-derived growth factor (PDGF) D, where *n*=3. Control (CTRL) and mock samples were not transfected. Migration was assessed by cell assay, where mock was stimulation control (a-c). Values are means ± SEM. An unpaired Students *t*-test was used to determine *P*-values. +++++ = 95% of gap area covered by fibroblasts, ++++ = 90% of gap area covered by fibroblasts, +++= 85% of gap area covered by fibroblasts. Representative images shown in Appendix (**Fig. 23**)

5 Discussion

5.1 Summary of results

So far, little is known about the role miR-34a plays in lung development, however, it has been demonstrated that several miRNAs were deregulated after hyperoxia exposure of neonatal rat lungs and one of the most strikingly upregulated miRNAs was miR-34a [4]. This thesis is an attempt to shed some light on the role of miR-34a regulating fibroblast migration and therefore late lung development and BPD pathogenesis. To this end a series of in vitro experiments was performed, involving exposing MLg fibroblasts to hyperoxia and over expressing miR-34a in fibroblasts via transfection in order to examine its targets PDGFRα and PDGFRβ, its downstream signalling by means of Western Blot, and its impact on fibroblast migration per migration assay. The effect of miR-34a was therefore demonstrated on multiple levels of the miR-34a – PDGFR axis.

Exposing MLg fibroblasts to 85% O_2 resulted in upregulation of the entire miR-34 family, although the effect of hyperoxia was strongest in miR-34a. Additionally, PDGFRα and PDGFRβ protein levels were found to be downregulated after hyperoxia exposure. Then, transfecting MLg fibroblasts with a miR-34a mimic demonstrated a downregulation of both PDGFRα and PDGFRβ. In both experiments the downregulation of PDGFRα was stronger than the downregulation of PDGFRβ. Investigation of the downstream signalling molecules of PDGFRα and PDGFRβ, AKT and ERK initially showed no difference of activation after miR-34a over expression, however stimulating PDGFRα and PDGFRβ with their specific ligands, after miR-34a over expression showed some effect. After stimulation with PDGFA, both AKT and ERK activation were reduced, after stimulating with PDGFB and PDGFD, only ERK activation was decreased. AKT activation remained consistent **(table 7)**. Furthermore, the effect of miR-34a was shown on a functional level: miR-34a over expression significantly reduced fibroblast migration in a cell assay. The effect was amplified by stimulating fibroblasts with PDGF-A, PDGF-B and PDGF-D after miR-34a over-expression. Although some questions remain unanswered, this study was able to elucidate the role of miR-34a in regulating fibroblast migration by reducing PDGFR signalling.

Table 7: Summary of results miR-34a transfection of MLg fibroblasts and its effect on AKT and ERK

Fibroblasts stimulated with	Downregulation of AKT	Downregulation of ERK
PDGFA	Yes	Yes
PDGFB	No	Yes
PDGFD	No	Yes

5.2 Analysis of results

The results demonstrated by the hyperoxia experiment showed higher levels of the members of the miR-34 family, where miR-34a was upregulated more than miR-34b and miR-34c. These results are in accordance to the results presented by Bhaskaran and colleagues, in which miR-34a is upregulated in neonatal rat lungs that were exposed to hyperoxia using miRNA microarray and real-time qPCR. [4], the study did not research the effect of hyperoxia on miR-34b or miR-34c. Another study performed by Bommer and colleagues compared expression levels of the members of the miR-34 family in different organs of mice. It was revealed that although miR-34a was ubiquitously expressed at higher levels than miR-34b and miR-34c, miR-34b and miR-34c were expressed at around five times higher levels than miR-34a in lungs [71]. So even though miR-34a is less abundant than miR-34b and miR-34c in mouse lungs, the effect of hyperoxia on miR-34a is greater than on miR-34b and miR-34c, highlighting the importance of miR-34a as a response to hyperoxia exposure. The second hyperoxia experiment revealed that PDGFRα and PDGFRβ were downregulated after exposure to 85% O_2, demonstrating an inverse correlation between miR-34a expression and PDGFRα and PDGFRβ protein levels. These results match the findings of Garofalo and colleagues, which demonstrated an inverse correlation between miR-34a and PDGFRα and PDGFRβ expression in two lung cancer cell lines and in vivo in non-small cellular lung cancer (NSCLC) [76]. The results are also in congruence with the study performed by Popova and colleagues, which found that neonatal mesenchymal stromal cells (MSC) from infants who developed BPD, and were treated with mechanical ventilation, show lower mRNA and protein expression of PDGFRα and PDGFRβ [89].

Over-expression of miR-34a in MLg fibroblasts led to downregulation of PDGFRα and PDGFRβ protein levels, indicating miR-34a as a part of the mechanism driving hyperoxia induced PDGFRα and PDGFRβ downregulation. This idea is supported by the aforementioned study by Garofalo and colleagues, which also established that miR-34a targets PDGFRα and PDGFRβ mRNA directly at its 3' UTR [76]. Furthermore, the results from both hyperoxia treatment and miR-34a over-expression show that PDGFRα protein levels are brought down more than PDGFRβ protein levels. The reason for this difference in downregulation could be that the miR-34a seed sequence matches two regions on PDGFRα mRNA (nucleotides 2670-2676 and nucleotides 2699 and 2705) but only one region on PDGFRβ mRNA (nucleotides 1535-1541) [76], suggesting that miR-34a has twice as many binding sites, on PDGFRα mRNA than on PDGFRβ mRNA, thus influencing PDGFRα more effectively than PDGFRβ. This research further supports the theory, that miR-34a upregulation causes PDGFRα and PDGFRβ downregulation in hyperoxia.

To further investigate the effect of miR-34a on PDGFRα and PDGFRβ, the activation of AKT and ERK, two downstream signalling molecules [81], were examined after miR-34a over-expression in fibroblasts. The western blot analysis showed no significant alteration in AKT and ERK activation, even though a transfection control confirmed successful transfection. Because miR-34a over-expression resulted in PDGFRα and PDGFRβ downregulation, the expected results were that the PDGFRα and PDGFRβ downstream signalling molecules AKT and ERK would be equally downregulated. It is not entirely clear why the expected results were not obtained, although it is suspected, that the downstream signalling of PDGFRα and PDGFRβ was not affected, because the receptors were in an inactivated state. This idea is supported by the changes in downstream signalling that were obtained when stimulating the receptors with their respective ligands. Alternatively, or additionally contributing to these results could be that even though AKT and ERK are downstream signalling molecules of PDGFRα and PDGFRβ, they are not exclusively activated by PDGFRs [97]. This leads to the idea that miR-34a may directly or indirectly affect another molecule, which in turn activates AKT and ERK, thus masking the expected effect on PDGFR downstream signalling. This idea is supported by the known fact, that miRNAs are able to affect many different targets,

due to short seed sequences and imperfect complementarity [42]. Furthermore, the mechanisms of miR-34a are yet to be fully understood.

Keeping in mind that AKT and ERK are not specific for the PDGFRs, in addition to miR-34a over-expression, the fibroblasts were treated with PDGFA, PDGFB and PDGFD, in order to investigate the effect of miR-34a on PDGFR downstream signalling. The results from stimulating PDGFRα and PDGFRβ with their ligands each revealed a significant reduction of activated ERK, whereas the activation of AKT was only also reduced after stimulation with PDGFA. Stimulation with PDGFB and PDGFD after miR-34a over-expression showed no change in AKT activation **(table 7).** Therefore only stimulating PDGFRα with its specific ligand PDGFA [79] resulted in reduced levels of both activated ERK and AKT after miR-34a over-expression, leading to the assumption that miR-34a affects PDGFR downstream signalling primarily through PDGFRα. This theory compares well with the previous results obtained in this thesis: Hyperoxia and miR-34a over expression seem to affect PDGFRα more strongly than PDGFRβ. However, when stimulating with PDGFB, which is the ligand for both PDGFRα and PDGFRβ [79], only ERK, but not AKT was affected by miR-34a over-expression. Similar results were obtained when stimulating with PDGFD, which mostly binds PDGFRβ [66], although research suggests that PDGFD also binds to the PDGFRα and PDGFRβ heterodimer [96], thus also activating PDGFRα. In this series of stimulation experiments there are two common features in each result: Firstly, ERK activation is reduced after stimulating with PDGFA, PDGFB and PDGFD, all stimulating PDGFRα at least to some extent. Secondly, in each case PDGFRβ was stimulated, the results showed that AKT activation is not affected by miR-34a over-expression, further consolidating the idea that miR-34a affects PDGFR downstream signalling mainly through PDGFRα. The missing downregulation of activated AKT in miR-34a over-expressing fibroblasts after stimulation of PDGFRβ leads to the speculation that AKT is activated by other molecules also affected by miR-34a. Even though some open questions remain, this therefore demonstrates that miR-34a over-expression impacts not only PDGFR protein expression, but also its downstream signalling, most likely mainly through PDGFRα.

Considering the involvement of AKT in fibroblast migration and of ERK in fibroblast proliferation [94, 95] this data suggests that miR-34a regulates fibroblast migration mainly via PDGFRα, which is also more strongly affected by miR-34a. The extent of the

involvement of PDGFRβ is not entirely clarified by these experiments. On the one hand PDGFRβ is clearly downregulated by miR-34a over expression, on the other hand the downstream signalling of PDGFRβ is not as strongly affected as the downstream signalling of PDGFRα. Especially the lack of AKT downregulation after miR-34a over expression suggests a more minor role of PDGFRβ, taking into account the implied importance of AKT in fibroblast migration [95]. Also to be considered is that it is unclear whether PDGFD is a specific ligand to PDGFRβ. While one study reports it to be the specific ligand to PDGFRβ [80], another reports PDGFD to also bind to the PDGFRα/β heterodimer [96]. Therefore, it remains uncertain whether the downregulation of ERK activation caused by miR-34a is to be attributed to PDGFRβ alone when stimulated with PDGFD.

To investigate the effect of miR-34a on a functional level, migration assays were performed, first without, then with stimulating PDGFRα and PDGFRβ with their ligands. In the migration assay without PDGFR stimulation, migration in miR-34a over expressing MLg fibroblasts was significantly reduced after 48h. There was no significant difference after 24h. However, whether PDGFRα and PDGFRβ are part of the process that reduces migration after miR-34a over-expression remained unclear. In order to connect miR-34a induced inhibition of fibroblast migration and the PDGFRs, the miR-34a over-expressing fibroblasts were stimulated with PDGFA, PDGFB and PDGFD in different migration assays. In the migration assays, in which the fibroblasts were treated with PDGF, migration of miR-34a over-expressing fibroblasts was already reduced after 24h, showing an earlier decrease in migration than without stimulating PDGFRα and PDGFRβ. These findings are in concurrence with the results from the PDGF treated western blots for AKT and ERK. After 24 h of transfection, AKT and ERK showed no reduction in activation without PDGF stimulation, however when treated with PDGF, downstream signalling is significantly reduced in miR-34a transfected fibroblasts. This shows a link between miR-34a, the PDGFR, their downstream signalling, and fibroblasts migration. Furthermore, since PDGFA is the specific ligand for PDGFRα, PDGFB binds both PDGFRα and PDGFRβ [79], it therefore shows, that miR-34a reduces fibroblast migration by downregulating PDGFRα. Whether mir-34a curbs fibroblast migration through PDGFRβ downregulation remains unanswered because of the aforementioned additional binding of PDGFD to the PDGFRα/β heterodimer [80, 96]. The role of

PDGFRβ in late lung development demands further research, but these results highlight the importance of miR-34a and PDGFR signalling in the development of BPD, considering the importance of fibroblast migration in alveolarization and thus late lung development.

Returning to the PDGFD stimulated western blot for AKT and ERK, an unexpected result was, that stimulating MLg fibroblasts with PDGFD alone, as stimulation control, caused a decrease in ERK activation. Similar results can be found in the PDGFD stimulated migration assay, where stimulation with PDGFD alone, caused fibroblasts to migrate less, than the fibroblasts that were not stimulated with PDGFD. Considering the role of PDGFD and its receptors, these results seem contradictory, to what would be expected. Although it is unclear why, a possible explanation would be a negative feedback loop, reducing ERK activation and therefore fibroblast migration. It also could be a currently unknown effect of PDGFRβ, since PDGFD mainly stimulates PDGFRβ. The reduced downstream signalling and fibroblast migration in miR-34a over expressing fibroblasts could be the effect of PDGFD also stimulating PDGFRα through the PDGFRα/β heterodimer to some extent. This further supports the theory, that miR-34a mainly reduces fibroblast migration via PDGFRα, rather than PDGFRβ. Because these unexpected results were obtained from the stimulation control from both the PDGFD stimulated western blot and migration assay, it sheds a different light on its main results. These were, that ERK activation and fibroblast migration is reduced in miR-34a over expressing fibroblasts, when stimulated with PDGFD. However, since the stimulation control showed this particular data, a conclusive statement regarding ERK activation and fibroblast migration in miR-34a over expressing fibroblasts in not possible. Since those results were obtained repeatedly, an error in method was ruled out.

5.3 Open questions and Outlook

Prior to the begin of the thesis, primary mouse lung fibroblasts had demonstrated a poor resistance to hyperoxia in the laboratory. However, MLg fibroblasts, a mouse lung cell line, showed strong resilience in extreme conditions such as hyperoxia, therefore the MLg cell line was chosen for further investigation. Thus, an open question remaining is whether similar results can be obtained when investigating primary mouse lung fibroblasts and primary human fibroblasts. A different study researching BPD was able to detect sex-specific differences in BPD and in miR-34a expression using primary mouse

lung fibroblasts [98] Another study researching BPD by Syed et al. also showed increased levels of miR-34a in primary AEC type 2 cells and in a cell line: Mouse lung epithelial (MLE) 12. Differently to this thesis, the primary AEC type 2 cells were exposed to hyperoxia for a shorter time: 4h and 16h, in comparison to 24h and 48h [99]. Although it is still unclear, these findings indicate, that similar results would have been obtained, if primary lung fibroblasts would have been used, instead of the cell line used for this thesis. Perhaps a shorter time of exposure to hyperoxia, could have made experiments possible in primary lung fibroblasts. In Addition to the results listed above, Syed et al. showed increased levels of miR-34a in tracheal aspirates of human neonates with BPD or RDS. These results in Human BPD therefore validate the relevance of not only their own research on mice, but also the research done in this thesis.

Another open question remaining is, if similar results would have been obtained when transfecting MLg fibroblasts with miR-34b and miR34c instead of miR-34a. MiR-34a was chosen to be investigated because it showed the strongest reaction to hyperoxia in comparison to miR-34b and miR-34c. However, in previous research, it was revealed that miR-34b and miR-34c are expressed at around five times more in lungs than miR-34a [71]. Even though miR-34b and miR-34c showed a less strong reaction to hyperoxia than miR-34a, this could indicate an important role for miR34b and miR34c. Whether it is an important role in fibroblast migration involving the PDGF receptors is still unclear. So far, miR-34b and c have not extensively been investigated in BPD, yet some research has been made regarding NSCLC. Both miR-34b and c have been shown to inhibit migration and proliferation of NSCLC cell lines [100, 101]. More specifically, miR-34c was proven to reduce proliferation and invasion of NSCLC cell lines via mitogen-activated protein (MAP) kinase [101]. Keeping in mind, that ERK belongs to the family of MAP kinases, this indicates that the miR-34 family targets similar pathways to regulate migration. To conclude, even though the research has been made in NSCLC cell lines, miR-34b and c have been shown to reduce migration of said cells, even by similar mechanisms. This imposes the idea, that similar results would have been obtained, when transfecting MLg fibroblasts with miR-34b or c, instead of miR-34a.

In the analysis of the results it was already theorized that miR-34a affects PDGF receptor downstream signalling mainly through PDGFRα, because of the lack of reduction of activated AKT when stimulating PDGFRβ. What still remains unclear is the exact reason for this. Considering that AKT is not specific for the PDGF receptors, the assumption is

that PDGFRβ, when stimulated, activates a different molecule, which in turn then activates AKT, masking the downregulation of AKT via miR-34a. Furthermore, miR-34a targets many different molecules that could interfere with the activation of AKT and ERK. For example, in the aforementioned study by Syed et al., miR-34a was shown to reduce angiopoetin-1 expression, which binds to the tyrosine kinase Tie2, which in turn activates AKT and MAP kinase in AEC type 2 cells of hyperoxia treated rat lungs [99]. This indicates that the lack of decreased activation of AKT in miR-34a over expressing fibroblasts could be a cause of different molecules being activated by miR-34a.

One of the main open questions remaining is the role of PDGFRβ and whether it is part of the miR-34a – PDGFR axis curbing fibroblast migration. The methods used in thesis were merely able to hint at an involvement of PDGFRβ, however it could not fully elucidate its role. Since it is unclear whether PDGFD is a specific ligand to PDGFRβ or whether it also binds to the PDGFRα/β heterodimer [80, 96], it is uncertain if downstream signalling and fibroblast migration would be downregulated in miR-34a over expressing fibroblasts if PDGFRβ exclusively had been stimulated. A more promising approach to reveal the extent of its involvement in fibroblast migration could be to involve small interfering RNAs (siRNA). Using a specific siRNA to block PDGFRα expression in miR-34a transfected fibroblasts could further elucidate the role of PDGFRβ in fibroblast migration. So far, PDGFRβ has not extensively been investigated in BPD. However, a study by de Visser et al., showed that apelin, a potent vasodilator and angiogenic factor, attenuates hyperoxic lung injury in neonatal rats [102]. Although PDGFRβ was not a target of this investigation, different studies examining Apelin in context of liver fibrosis discovered that apelin and the apelin receptor upregulate PDGFRβ [103]. Considering apelin targets PDGFRβ, and plays a role in hyperoxia induced lung injury, these connections hint at a role of PDGFRβ in BPD. Therefore, the function of PDGFRβ in BPD deserves further research.

This thesis was able to shed some light on the effect miR-34a has on fibroblast migration by modulating PDGFR signalling, however it merely set the groundwork required for further research on miR-34a and PDGFRα and PDGFRβ in late lung development. This research was able to show promising results indicating a prominent role of miR-34a and PDGFRα interaction in fibroblast migration, so that further research involving in vivo experiments in mice were conducted. In a hyperoxia induced model of BPD in mice,

different ways of targeting miR-34a and its interaction with PDGFRα were shown to restore alveolarization [104]. Since Syed et al. already showed increased levels of miR-34a in human BPD [99], miR-34a should be looked at as a possible target for therapy of BPD.

Considering the prospect of future treatment options for BPD involving miR-34a and PDGFRα and PDGFRβ, there are different possibilities. Future medication for BPD could be antagonising miR-34a directly via complementary RNA-strands (Antagomir), or by specifically blocking the binding of mir-34a to the PDGF receptors using a target site blocker. Taking into account that miR-34a is expressed ubiquitously and that miR-34a affects many different targets, the most promising approach would be to interfere with the miR-34a – PDGF receptor interactions by the use of a target site blocker. This approach would be advantageous as to leaving other targets of miR-34a unaffected, whilst specifically inhibiting the pathophysiological interaction contributing to BPD. The approach had already been proven effective by partially restoring alveolarization in a hyperoxia induced mouse model by Ruiz-Camp et al [104]. Another approach for clinical application would be the application of PDGF in order to treat BPD. In a study by Oak et al. endotracheal application of PDGFA resulted in higher numbers of alveoli in a mouse model with mechanically ventilated mice versus the control. The study also showed an increase of micro vessels and PDGFRα expression in PDGFA treated mice [105]. To further specify the medication and to minimize possible side effects, a volatile administration form for pulmonal application of such medication would be preferable, as miR-34a and PDGFR are ubiquitously expressed.

Another future clinical prospect to be considered is miR-34a and the PDGF receptors as a predictive marker for BPD, furthermore it could find clinical application as prognostic marker regarding the severity of the disease. Even though there have been several efforts, so far, no marker has definitely established itself in clinical practise. However, some studies showed some promising results: Studies by Borghese and by Baker revealed low levels of endothelial colony forming cells (ECFC) in umbilical cord blood, for example CD34+, CD133-, CD45-, and vascular endothelial growth factor (VEGF) receptor, were associated with an increased risk of developing BPD [106, 107]. Another study showed, that low levels of VEGF in tracheal fluid of preterm infants also correlated with the occurrence of BPD [108]. Further potential predictive markers are also Clara cell protein (CC) 16 and KL-6, a serum marker for interstitial lung disease, were used in as a

combination to predict the occurrence of BPD [109]. A study by Tokuriki et al. claimed carboxyhaemoglobin (CO-Hb) as predictive marker for BPD [110]. As it is easy to measure in the blood of preterm infants, this approach seems to be the most feasible for clinical practice. However, CO-Hb can be influenced by many factors, such as infection and sepsis [111], and therefore has not been established as a marker for BPD in clinical practice. A more recent study revealed, that high levels of oxylipins, for example Prostaglandin E (PGE) 1 and 2, not only correlated with the occurrence of BPD, but also showed prospect as a prognostic marker for the severity of the disease [112]. Nonetheless, it has yet to be implemented into clinical practice. Therefore, BPD lacks a reliable marker to predict its occurrence and to predict the severity of the disease, even though promising efforts have been made. Whether miR-34a or the PDGF receptors have any value as predictive markers is unknown so far, and deserves further investigation.

6 Summary

Bronchopulmonary dysplasia (BPD) is a chronic lung disease, which often occurs in preterm infants due to neonatal lung injury, and is defined by a lack of alveoli formation. Depending on the severity of the disease there are severe long-term consequences, such as early onset of chronic obstructive lung disease (COPD). Although a lot of progress has been made to improve the outcome of the disease, a cure has yet to be found. Therefore, it is imperative to investigate the development of BPD in order to identify new targets to improve the prognosis of the disease. In an experimental mouse model of hyperoxia induced BPD, a microarray showed an upregulation of microRNA (miR)-34a. It was also revealed, that miR-34a targets the platelet-derived growth factor receptors (PDGFR) α and β, which are known to be crucial for fibroblast migration during secondary septation. Downstream signalling molecules of PDGFRα and β are for example extracellular signal-regulated kinase (ERK) and AKT, also known as Protein Kinase B.

In this thesis, a series of in vitro experiments including real-time quantitative polymerase chain reaction (qPCR), transfection, western blot analysis and migration assay, was conducted in mouse lung (MLg) fibroblasts, to investigate the effect of miR-34a on PDGFRα and β and on fibroblast migration. It was revealed by qPCR analysis that hyperoxia firstly increases the level of the miR-34 family, most notably of miR-34a, and secondly reduces the expression of PDGFRα and β in MLg fibroblasts. Transfecting MLg

fibroblasts with miR-34a also showed a reduction of PDGFRα and β levels. To further examine the effects of miR-34a on PDGFRα and β, its downstream signalling molecules were investigated. Western blot analysis showed a reduced activation of downstream signalling, especially when stimulating the miR-34a transfected MLg fibroblasts with PDGFA, the specific ligand to PDGFRα. Furthermore, migration assays revealed reduced migration in MLg fibroblasts after miR-34a transfection, with and without stimulation of PDGFRα and β with their ligands.

In conclusion, these results suggest an important role of miR-34a as a negative regulator of fibroblasts migration via the PDGFR, and thus as a crucial factor in one of the mechanisms causing BPD. Therefore, further investigation of miR-34a and PDGFR interaction could contribute to a deeper understanding of BPD and ultimately improve the outcome of the disease.

7 Zusammenfassung

Bronchopulmonale Dysplasie (BPD) ist eine chronische Erkrankung der Lunge, die häufig bei Frühgeborenen auftritt, die einer künstlichen Beatmung bedürfen. Die Erkrankung ist durch einen Mangel an Alveolen charakterisiert. Abhängig vom Schweregrad der Erkrankung gibt langfristige Komplikationen, zum Beispiel frühes Einsetzen von chronisch obstruktiver Lungenerkrankung (COPD). Obwohl bereits viele Fortschritte gemacht wurden um das Outcome der Erkrankung zu verbessern, konnte diese Erkrankung bisher nicht geheilt werden. Daher ist es notwendig die Entstehung von BPD zu untersuchen, um neue Therapietargets zu identifizieren, um die Prognose der Erkrankung zu verbessern. In einem experimentellen Mausmodell mit Hyperoxie induzierter BPD, konnte eine vermehrte Expression von microRNA (miR)-34a festgestellt werden. Ferner wurde festgestellt, dass platelet-derived growth factor receptor (PDGFR) α und β, wichtige Moleküle für die Migration von Fibroblasten, Targets von miR-34a sind. Nachgeschaltete Signalmoleküle von PDGFRα und β sind zum Beispiel extracellular regulated kinase (ERK) und AKT, auch bekannt als Protein Kinase B.

In dieser Arbeit wurden mittels einer Serie von Zellversuchen an Mauslungen (MLg) Fibroblasten die Effekte von miR-34a auf PDGFRα und β und auf Fibroblasten Migration untersucht. Diese Versuche beinhalteten quantitative Echtzeit-Polymerase-

Kettenreaktion (qPCR), Transfektion, Western Blot Analyse und Migrationsassays. Es konnte mittels qPCR gezeigt werden, dass Hyperoxie erstens die Expression der miR-34 Familie, vor allem von miR-34a, verstärkt, und zweitens, die Expression von PDGFRα und β reduziert. Eine Transfektion der MLg Fibroblasten zeigte ebenso eine Reduktion von PDGFRα und β Expression. Um die Wirkung von miR-34a auf PDGFRα und β tiefgründiger zu untersuchen, wurden dessen nachgeschaltete Signalmoleküle untersucht. Western Blot Analyse zeigte eine reduzierte Aktivierung dieser Signalmoleküle in mit miR-34a transfizierten MLg Fibroblasten, insbesondere in dem Fall einer Stimulation mit PDGFA, dem spezifischen Liganden für PDGFRα. Des Weiteren konnten mittels Migrationsassays eine reduzierte Migration der miR-34a transfizierten MLg Fibroblasten festgestellt werden, mit und ohne Stimulation von PDGFRα und β mit ihren Liganden.

Zusammenfassend deuten diese Ergebnisse auf eine wichtige Rolle von miR-34a als negativer Regulator von Fibroblasten-migration durch die PDGFR, und somit als Teil einer der Mechanismen, die die Entstehung von BPD begünstigen. Daher könnte weitere Forschung an der miR-34a und der PDGFRα und β das Verständnis der Pathophysiologie von BPD vertiefen und letztlich zu einer Verbesserten Prognose der Erkrankung führen.

8 Additional Data

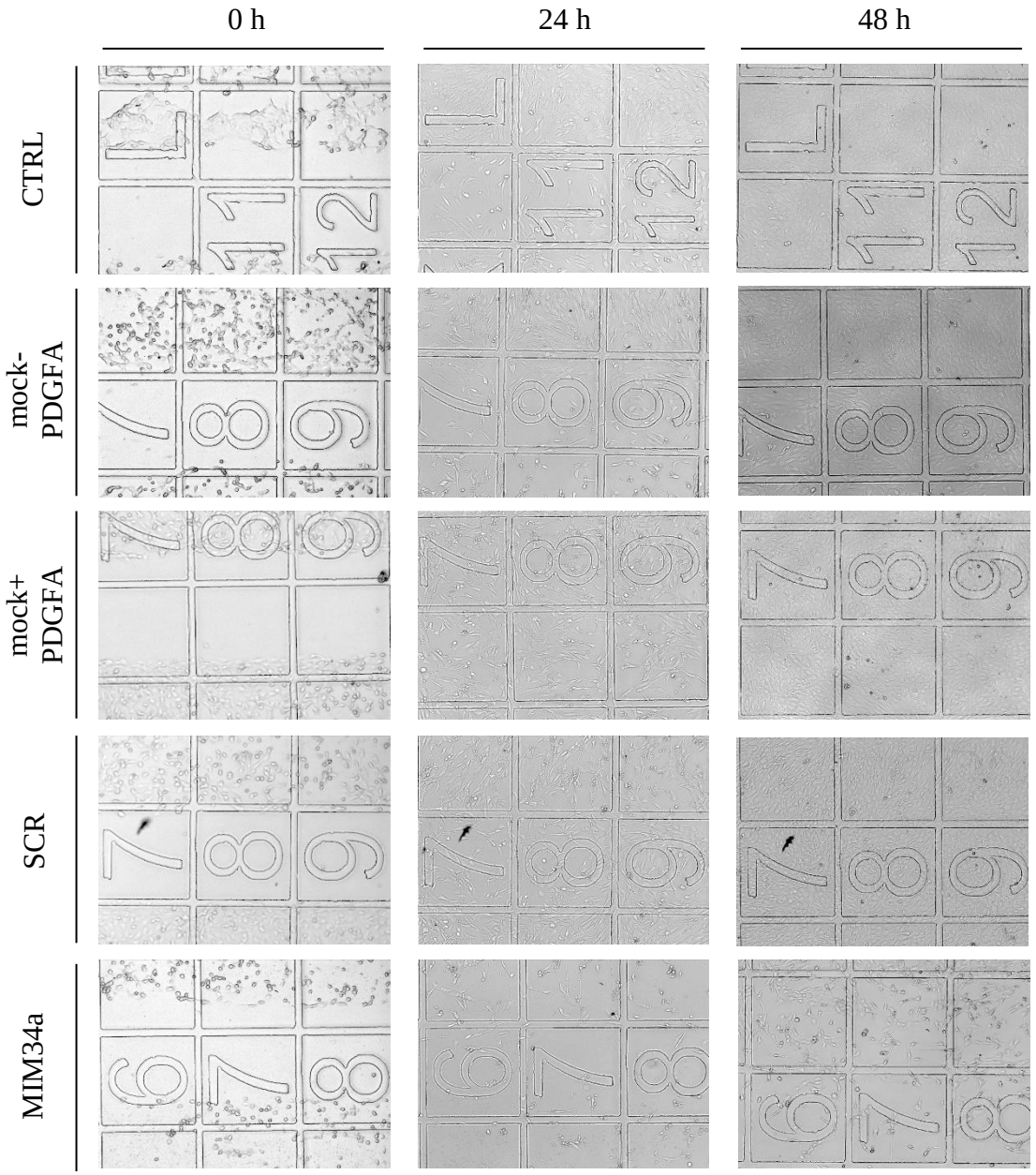

Figure 22. Over expression of mirRNA-34a inhibits migration in PDGFA treated fibroblasts after 24 h and after 48 h (representative images). Analysis of data shown in Results (Fig. 18). Mouse lung (MLg) fibroblasts were transfected with 80nM scrambled microRNA (SCR) and microRNA-34a mimic (MIM34a) for 24 h, and stimulated with platelet-derived growth factor (PDGF) A, where *n*=3. Control (CTRL) and mock samples were not transfected. Migration was assessed by cell assay, where mock was stimulation control.

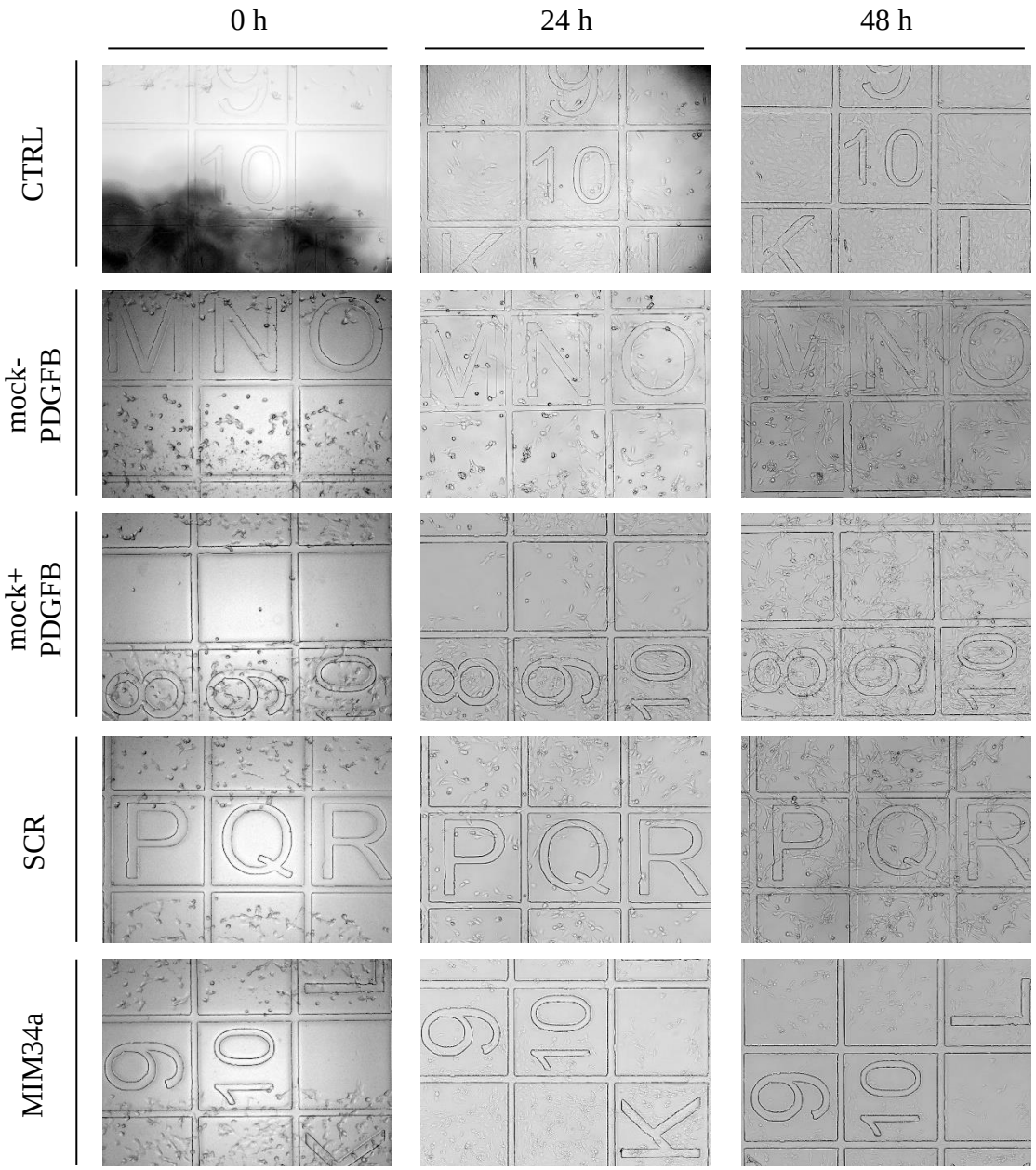

Figure 23. Over expression of miRNA-34a inhibits migration in PDGFB treated fibroblasts after 24 h and after 48 h (representative images). Analysis of data shown in Results (Fig. 19). Mouse lung (MLg) fibroblasts were transfected with 80nM scrambled microRNA (SCR) and microRNA-34a mimic (MIM34a) for 24 h, and stimulated with platelet-derived growth factor (PDGF) B, where *n*=3. Control (CTRL) and mock samples were not transfected. Migration was assessed by cell assay, where mock was stimulation control.

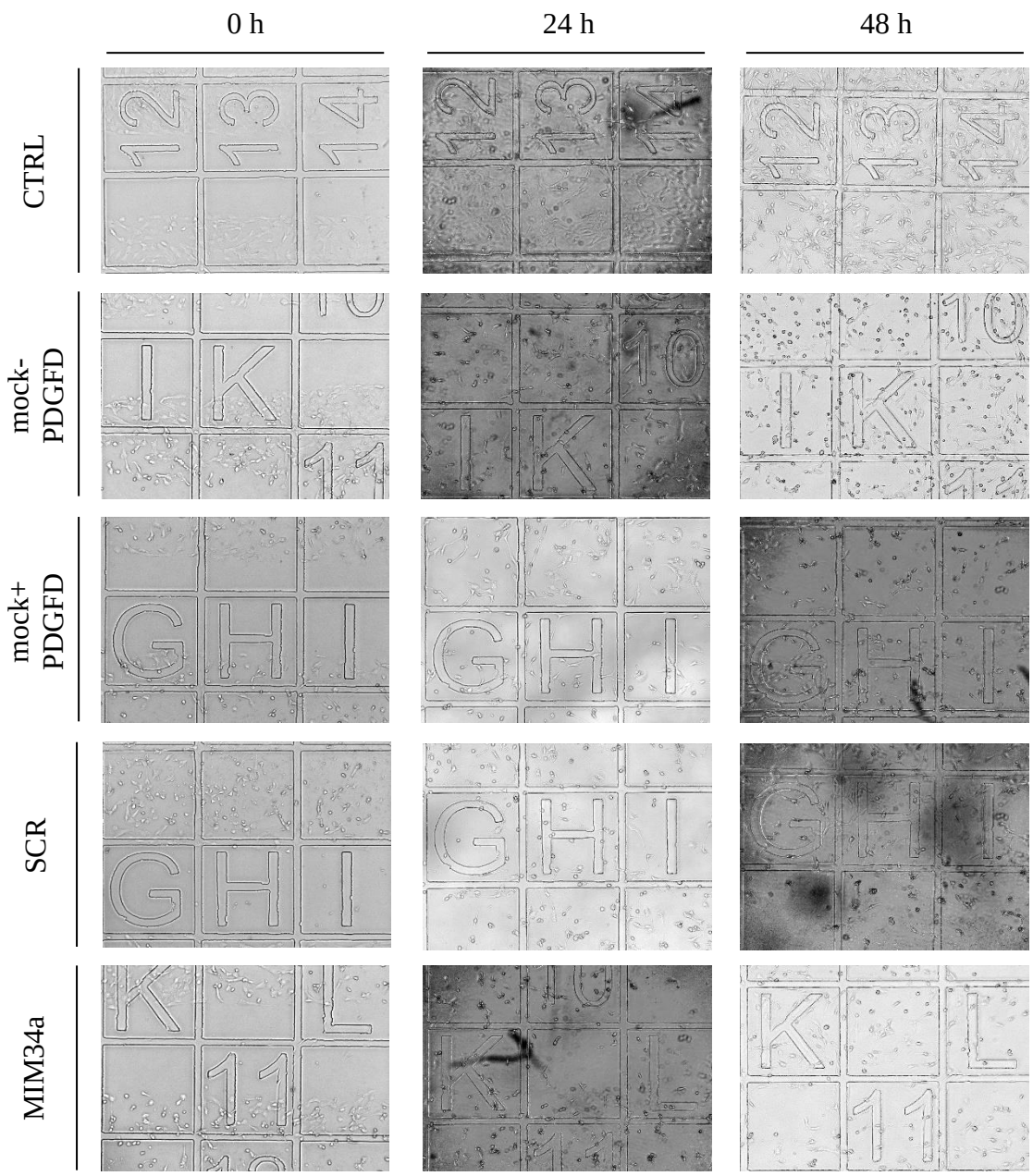

Figure 24. Over expression of miRNA-34a inhibits migration in PDGFD treated fibroblasts after 24 h and after 48 h (representative images). Analysis of data shown in Results (Fig. 20). Mouse lung (MLg) fibroblasts were transfected with 80nM scrambled microRNA (SCR) and microRNA-34a mimic (MIM34a) for 24 h, and stimulated with platelet-derived growth factor (PDGF) D, where *n*=3. Control (CTRL) and mock samples were not transfected. Migration was assessed by cell assay, where mock was stimulation control.

9 List of abbreviations

[c]	Concentration
°C	Degrees Celsius
ADAR	Adenosine deaminases acting on RNA
AEC	Alveolar epithlial cell
α-sma	α-smooth muscle actin
BADJ	Bronchoalveloar duct junction
BPD	Bronchopulmonary dysplasia
BSA	Bovine serum albumine
CC	Clara cell protein
Chr	Chromosome
cm	Centimeter
CO_2	Carbondioxide
CO-Hb	Carboxyhaemoglobin
COPD	Chronic obstructive pulmonary disease
CTRL	Control
ΔC_T	Delta cycle threshold
DGCR	DiGeorge critical region
dH_2O	Destilled water
DMSO	Dimethylsulfoxide
DTT	Dithiothreitol
E	Embryonic day
ECFC	Endothelial colony-forming cells
ECM	Extra cellular matrix
EDTA	Ethylenediaminetetraacetic acid
EGTA	Ethylene glycol tetraacetic acid
EMEM	Eagle's mimimal essential medium
ERK	Extracellular signal-regulated kinase
FBS	Foetal bovine serum
g	Gram
g	Force of gravity

Grb	Protein activator of PKR
h	Hour/Hours
HCL	Hydrochloric acid
kDa	Kilodalton
KL-6	Krebs von den Lungen-6
l	Liter
MAP	Mitogen-activated Protein
µg	Microgram
µl	Microliter
µM	Micromole
mg	Milligram
MIM	MicroRNA mimic
min	Minutes
miR	MicroRNA
ml	Milliliter
MLE	Mouse lung epithelial
MLg	Mouse lung
mRNA	messenger RNA
MSC	Mesenchymal stromal cells
n	Number of cells
NaCl	Sodium chloride
NaOH	Sodiumhydroxide
ng	Nanogram
NICHD	National Institute of Child Health and Human Development
Nkx2-1	NK2 Homeobox 1
nm	Nanometer
NSCLC	Non-small cellular lung cancer
O_2	Oxygen
P	Post-natal day
P	Probability
PACT	Protein activator of PKR
PBS	Phosphate-buffered saline

PDGF	Platelet-derived growth factor
PDGFR	Platelet-derived growth factor receptor
PEEP	Positive end-expiratory pressures
PGE	Prostaglandin E
PI3K	Phosphoinositide-3-kinase
PMA	Postmenstrual age
qPCR	Real-Time quantitative polymerase chain reaction
RDS	Respiratory distress syndrome
RISC	RNA-induced silencing complex
RNA	Ribonucleic acid
SC	Standad curve solution
SCR	Scramble
SDS	Sodium dodecyl sulfat
SEM	Standart error
siRNA	Small interfering RNA
Sos	Son of sevenless
TEMED	N,N,N´,N´-Tetramethylethylenediamine
TGF	Transforming growth factor
™	Trademark
TRBP	Proteins Tar RNA binding protein
UTR	Untranslated region
V	Volt
VEGF	Vascular endothelial growth factor
v/v	Volume density
VLBW	Very low birth weight
XPO	Exportin

10 List of figures

11 List of tables

12 Bibliography

1. Ali, Z., et al., *Bronchopulmonary dysplasia: a review.* Arch Gynecol Obstet, 2013. **288**(2): p. 325-33.
2. Abman, S.H., *Bronchopulmonary dysplasia: "a vascular hypothesis".* Am J Respir Crit Care Med, 2001. **164**(10 Pt 1): p. 1755-6.
3. Walsh, M.C., et al., *Summary proceedings from the bronchopulmonary dysplasia group.* Pediatrics, 2006. **117**(3 Pt 2): p. S52-6.
4. Bhaskaran, M., et al., *Identification of microRNAs changed in the neonatal lungs in response to hyperoxia exposure.* Physiol Genomics, 2012. **44**(20): p. 970-80.
5. Rawlins, E.L., *The building blocks of mammalian lung development.* Dev Dyn, 2011. **240**(3): p. 463-76.
6. Burri, P.H., *Fetal and postnatal development of the lung.* Annu Rev Physiol, 1984. **46**: p. 617-28.
7. Morrisey, E.E. and B.L. Hogan, *Preparing for the first breath: genetic and cellular mechanisms in lung development.* Dev Cell, 2010. **18**(1): p. 8-23.
8. Alescio, T. and A. Cassini, *Induction in vitro of tracheal buds by pulmonary mesenchyme grafted on tracheal epithelium.* J Exp Zool, 1962. **150**: p. 83-94.
9. Winter, J., et al., *Many roads to maturity: microRNA biogenesis pathways and their regulation.* Nat Cell Biol, 2009. **11**(3): p. 228-34.
10. Hogan, B.L., et al., *Repair and regeneration of the respiratory system: complexity, plasticity, and mechanisms of lung stem cell function.* Cell Stem Cell, 2014. **15**(2): p. 123-38.
11. El Agha, E. and S. Bellusci, *Walking along the Fibroblast Growth Factor 10 Route: A Key Pathway to Understand the Control and Regulation of Epithelial and Mesenchymal Cell-Lineage Formation during Lung Development and Repair after Injury.* Scientifica (Cairo), 2014. **2014**: p. 538379.
12. Chao, C.M., et al., *A breath of fresh air on the mesenchyme: impact of impaired mesenchymal development on the pathogenesis of bronchopulmonary dysplasia.* Front Med (Lausanne), 2015. **2**: p. 27.
13. Sirianni, F.E., F.S. Chu, and D.C. Walker, *Human alveolar wall fibroblasts directly link epithelial type 2 cells to capillary endothelium.* Am J Respir Crit Care Med, 2003. **168**(12): p. 1532-7.
14. Weibel, E.R., *It takes more than cells to make a good lung.* Am J Respir Crit Care Med, 2013. **187**(4): p. 342-6.
15. Buczynski, B.W., E.T. Maduekwe, and M.A. O'Reilly, *The role of hyperoxia in the pathogenesis of experimental BPD.* Semin Perinatol, 2013. **37**(2): p. 69-78.
16. Ehrenkranz, R.A., et al., *Validation of the National Institutes of Health consensus definition of bronchopulmonary dysplasia.* Pediatrics, 2005. **116**(6): p. 1353-60.
17. Jobe, A.H. and E. Bancalari, *Bronchopulmonary dysplasia.* Am J Respir Crit Care Med, 2001. **163**(7): p. 1723-9.
18. Farstad, T., et al., *Bronchopulmonary dysplasia - prevalence, severity and predictive factors in a national cohort of extremely premature infants.* Acta Paediatr, 2011. **100**(1): p. 53-8.

19. Carey, M.A., et al., *The impact of sex and sex hormones on lung physiology and disease: lessons from animal studies.* Am J Physiol Lung Cell Mol Physiol, 2007. **293**(2): p. L272-8.
20. Bhandari, V., et al., *Familial and genetic susceptibility to major neonatal morbidities in preterm twins.* Pediatrics, 2006. **117**(6): p. 1901-6.
21. Lahra, M.M., P.J. Beeby, and H.E. Jeffery, *Intrauterine inflammation, neonatal sepsis, and chronic lung disease: a 13-year hospital cohort study.* Pediatrics, 2009. **123**(5): p. 1314-9.
22. *Supplemental Therapeutic Oxygen for Prethreshold Retinopathy Of Prematurity (STOP-ROP), a randomized, controlled trial. I: primary outcomes.* Pediatrics, 2000. **105**(2): p. 295-310.
23. Warner, B.B., et al., *Functional and pathological effects of prolonged hyperoxia in neonatal mice.* Am J Physiol, 1998. **275**(1 Pt 1): p. L110-7.
24. Freeman, B.A. and J.D. Crapo, *Biology of disease: free radicals and tissue injury.* Lab Invest, 1982. **47**(5): p. 412-26.
25. Ikegami, M. and A.H. Jobe, *Injury responses to different surfactants in ventilated premature lamb lungs.* Pediatr Res, 2002. **51**(6): p. 689-95.
26. Wada, K., A.H. Jobe, and M. Ikegami, *Tidal volume effects on surfactant treatment responses with the initiation of ventilation in preterm lambs.* J Appl Physiol (1985), 1997. **83**(4): p. 1054-61.
27. Naik, A.S., et al., *Effects of ventilation with different positive end-expiratory pressures on cytokine expression in the preterm lamb lung.* Am J Respir Crit Care Med, 2001. **164**(3): p. 494-8.
28. Short, E.J., et al., *Cognitive and academic consequences of bronchopulmonary dysplasia and very low birth weight: 8-year-old outcomes.* Pediatrics, 2003. **112**(5): p. e359.
29. Teune, M.J., et al., *Perinatal risk-indicators for long-term respiratory morbidity among preterm or very low birth weight neonates.* Eur J Obstet Gynecol Reprod Biol, 2012. **163**(2): p. 134-41.
30. Wheeler, K.I., et al., *Volume-targeted versus pressure-limited ventilation for preterm infants: a systematic review and meta-analysis.* Neonatology, 2011. **100**(3): p. 219-27.
31. Network, S.S.G.o.t.E.K.S.N.N.R., et al., *Target ranges of oxygen saturation in extremely preterm infants.* N Engl J Med, 2010. **362**(21): p. 1959-69.
32. Crowley, P.A., *Antenatal corticosteroid therapy: a meta-analysis of the randomized trials, 1972 to 1994.* Am J Obstet Gynecol, 1995. **173**(1): p. 322-35.
33. Jobe, A.H., *Antenatal factors and the development of bronchopulmonary dysplasia.* Semin Neonatol, 2003. **8**(1): p. 9-17.
34. Yoder, M.C., Jr., R. Chua, and R. Tepper, *Effect of dexamethasone on pulmonary inflammation and pulmonary function of ventilator-dependent infants with bronchopulmonary dysplasia.* Am Rev Respir Dis, 1991. **143**(5 Pt 1): p. 1044-8.
35. Halliday, H.L., R.A. Ehrenkranz, and L.W. Doyle, *Early (< 8 days) postnatal corticosteroids for preventing chronic lung disease in preterm infants.* Cochrane Database Syst Rev, 2010(1): p. CD001146.
36. Henderson-Smart, D.J. and A.G. De Paoli, *Methylxanthine treatment for apnoea in preterm infants.* Cochrane Database Syst Rev, 2010(12): p. CD000140.

37. Schmidt, B., et al., *Evidence-based neonatal drug therapy for prevention of bronchopulmonary dysplasia in very-low-birth-weight infants.* Neonatology, 2008. **93**(4): p. 284-7.
38. Tyson, J.E., et al., *Vitamin A supplementation for extremely-low-birth-weight infants. National Institute of Child Health and Human Development Neonatal Research Network.* N Engl J Med, 1999. **340**(25): p. 1962-8.
39. Alphonse, R.S. and B. Thebaud, *Growth factors, stem cells and bronchopulmonary dysplasia.* Neonatology, 2011. **99**(4): p. 326-37.
40. Bartel, D.P., *MicroRNAs: genomics, biogenesis, mechanism, and function.* Cell, 2004. **116**(2): p. 281-97.
41. Friedman, R.C., et al., *Most mammalian mRNAs are conserved targets of microRNAs.* Genome Res, 2009. **19**(1): p. 92-105.
42. Dong, H., et al., *MicroRNA: function, detection, and bioanalysis.* Chem Rev, 2013. **113**(8): p. 6207-33.
43. He, L., et al., *A microRNA component of the p53 tumour suppressor network.* Nature, 2007. **447**(7148): p. 1130-4.
44. Kanellopoulou, C., et al., *Dicer-deficient mouse embryonic stem cells are defective in differentiation and centromeric silencing.* Genes Dev, 2005. **19**(4): p. 489-501.
45. Lee, Y., et al., *MicroRNA genes are transcribed by RNA polymerase II.* EMBO J, 2004. **23**(20): p. 4051-60.
46. Borchert, G.M., W. Lanier, and B.L. Davidson, *RNA polymerase III transcribes human microRNAs.* Nat Struct Mol Biol, 2006. **13**(12): p. 1097-101.
47. Kawahara, Y., et al., *Redirection of silencing targets by adenosine-to-inosine editing of miRNAs.* Science, 2007. **315**(5815): p. 1137-40.
48. Lee, Y., et al., *The nuclear RNase III Drosha initiates microRNA processing.* Nature, 2003. **425**(6956): p. 415-9.
49. Han, J., et al., *Molecular basis for the recognition of primary microRNAs by the Drosha-DGCR8 complex.* Cell, 2006. **125**(5): p. 887-901.
50. Yi, R., et al., *Exportin-5 mediates the nuclear export of pre-microRNAs and short hairpin RNAs.* Genes Dev, 2003. **17**(24): p. 3011-6.
51. Zeng, Y. and B.R. Cullen, *Structural requirements for pre-microRNA binding and nuclear export by Exportin 5.* Nucleic Acids Res, 2004. **32**(16): p. 4776-85.
52. Haase, A.D., et al., *TRBP, a regulator of cellular PKR and HIV-1 virus expression, interacts with Dicer and functions in RNA silencing.* EMBO Rep, 2005. **6**(10): p. 961-7.
53. Lee, Y., et al., *The role of PACT in the RNA silencing pathway.* EMBO J, 2006. **25**(3): p. 522-32.
54. MacRae, I.J., et al., *In vitro reconstitution of the human RISC-loading complex.* Proc Natl Acad Sci U S A, 2008. **105**(2): p. 512-7.
55. Khvorova, A., A. Reynolds, and S.D. Jayasena, *Functional siRNAs and miRNAs exhibit strand bias.* Cell, 2003. **115**(2): p. 209-16.
56. Liu, J., et al., *MicroRNA-dependent localization of targeted mRNAs to mammalian P-bodies.* Nat Cell Biol, 2005. **7**(7): p. 719-23.
57. Brennecke, J., et al., *bantam encodes a developmentally regulated microRNA that controls cell proliferation and regulates the proapoptotic gene hid in Drosophila.* Cell, 2003. **113**(1): p. 25-36.

58. Wang, Y., et al., *MicroRNAs in embryonic stem cells.* J Cell Physiol, 2009. **218**(2): p. 251-5.
59. Xu, P., et al., *The Drosophila microRNA Mir-14 suppresses cell death and is required for normal fat metabolism.* Curr Biol, 2003. **13**(9): p. 790-5.
60. Johnson, S.M., et al., *RAS is regulated by the let-7 microRNA family.* Cell, 2005. **120**(5): p. 635-47.
61. Thum, T., et al., *MicroRNAs in the human heart: a clue to fetal gene reprogramming in heart failure.* Circulation, 2007. **116**(3): p. 258-67.
62. Kapsimali, M., et al., *MicroRNAs show a wide diversity of expression profiles in the developing and mature central nervous system.* Genome Biol, 2007. **8**(8): p. R173.
63. Chen, C.Z., et al., *MicroRNAs modulate hematopoietic lineage differentiation.* Science, 2004. **303**(5654): p. 83-6.
64. Harris, K.S., et al., *Dicer function is essential for lung epithelium morphogenesis.* Proc Natl Acad Sci U S A, 2006. **103**(7): p. 2208-13.
65. Williams, A.E., et al., *Maternally imprinted microRNAs are differentially expressed during mouse and human lung development.* Dev Dyn, 2007. **236**(2): p. 572-80.
66. Lu, J., et al., *Differential expression of components of the microRNA machinery during mouse organogenesis.* Biochem Biophys Res Commun, 2005. **334**(2): p. 319-23.
67. Bhaskaran, M., et al., *MicroRNA-127 modulates fetal lung development.* Physiol Genomics, 2009. **37**(3): p. 268-78.
68. Lu, Y., et al., *Transgenic over-expression of the microRNA miR-17-92 cluster promotes proliferation and inhibits differentiation of lung epithelial progenitor cells.* Dev Biol, 2007. **310**(2): p. 442-53.
69. Hayashita, Y., et al., *A polycistronic microRNA cluster, miR-17-92, is overexpressed in human lung cancers and enhances cell proliferation.* Cancer Res, 2005. **65**(21): p. 9628-32.
70. Olave, N., et al., *Regulation of alveolar septation by microRNA-489.* Am J Physiol Lung Cell Mol Physiol, 2016. **310**(5): p. L476-87.
71. Griffiths-Jones, S., et al., *miRBase: microRNA sequences, targets and gene nomenclature.* Nucleic Acids Res, 2006. **34**(Database issue): p. D140-4.
72. Bommer, G.T., et al., *p53-mediated activation of miRNA34 candidate tumor-suppressor genes.* Curr Biol, 2007. **17**(15): p. 1298-307.
73. Yamamura, S., et al., *MicroRNA-34a modulates c-Myc transcriptional complexes to suppress malignancy in human prostate cancer cells.* PLoS One, 2012. **7**(1): p. e29722.
74. Yang, F., et al., *MicroRNA-34a targets Bcl-2 and sensitizes human hepatocellular carcinoma cells to sorafenib treatment.* Technol Cancer Res Treat, 2014. **13**(1): p. 77-86.
75. Lou, W., et al., *Oncolytic adenovirus co-expressing miRNA-34a and IL-24 induces superior antitumor activity in experimental tumor model.* J Mol Med (Berl), 2013. **91**(6): p. 715-25.
76. Garofalo, M., et al., *MiR-34a/c-Dependent PDGFR-alpha/beta Downregulation Inhibits Tumorigenesis and Enhances TRAIL-Induced Apoptosis in Lung Cancer.* PLoS One, 2013. **8**(6): p. e67581.
77. Boon, R.A., et al., *MicroRNA-34a regulates cardiac ageing and function.* Nature, 2013. **495**(7439): p. 107-10.

78. Johnsson, A., et al., *The c-sis gene encodes a precursor of the B chain of platelet-derived growth factor.* EMBO J, 1984. **3**(5): p. 921-8.
79. Heldin, C.H. and B. Westermark, *Mechanism of action and in vivo role of platelet-derived growth factor.* Physiol Rev, 1999. **79**(4): p. 1283-316.
80. Bergsten, E., et al., *PDGF-D is a specific, protease-activated ligand for the PDGF beta-receptor.* Nat Cell Biol, 2001. **3**(5): p. 512-6.
81. Montmayeur, J.P., et al., *The platelet-derived growth factor beta receptor triggers multiple cytoplasmic signaling cascades that arrive at the nucleus as distinguishable inputs.* J Biol Chem, 1997. **272**(51): p. 32670-8.
82. Valius, M. and A. Kazlauskas, *Phospholipase C-gamma 1 and phosphatidylinositol 3 kinase are the downstream mediators of the PDGF receptor's mitogenic signal.* Cell, 1993. **73**(2): p. 321-34.
83. Betsholtz, C., *Insight into the physiological functions of PDGF through genetic studies in mice.* Cytokine Growth Factor Rev, 2004. **15**(4): p. 215-28.
84. Gazit, A., et al., *Expression of the normal human sis/PDGF-2 coding sequence induces cellular transformation.* Cell, 1984. **39**(1): p. 89-97.
85. Porsch, H., et al., *Platelet-derived growth factor beta-receptor, transforming growth factor beta type I receptor, and CD44 protein modulate each other's signaling and stability.* J Biol Chem, 2014. **289**(28): p. 19747-57.
86. Bostrom, H., et al., *PDGF-A signaling is a critical event in lung alveolar myofibroblast development and alveogenesis.* Cell, 1996. **85**(6): p. 863-73.
87. Bostrom, H., A. Gritli-Linde, and C. Betsholtz, *PDGF-A/PDGF alpha-receptor signaling is required for lung growth and the formation of alveoli but not for early lung branching morphogenesis.* Dev Dyn, 2002. **223**(1): p. 155-62.
88. McGowan, S.E., et al., *Platelet-derived growth factor receptor-alpha-expressing cells localize to the alveolar entry ring and have characteristics of myofibroblasts during pulmonary alveolar septal formation.* Anat Rec (Hoboken), 2008. **291**(12): p. 1649-61.
89. Popova, A.P., et al., *Reduced platelet-derived growth factor receptor expression is a primary feature of human bronchopulmonary dysplasia.* Am J Physiol Lung Cell Mol Physiol, 2014. **307**(3): p. L231-9.
90 Cao, Y., R. Cao, and E.M. Hedlund, *R Regulation of tumor angiogenesis and metastasis by FGF and PDGF signaling pathways.* J Mol Med (Berl), 2008. **86**(7): p. 785-9.
91. Oates, T.W., et al., *Receptor binding of PDGF-AA and PDGF-BB, and the modulation of PDGF receptors by TGF-beta, in human periodontal ligament cells.* J Cell Physiol, 1995. **162**(3): p. 359-66.
92. Ibidi, *Ibidi Grid 500 plate: Instruction manual*, Martinsried, MA Author. **2015**.
93. Garofalo, M., et al., *Correction: MiR-34a/c-Dependent PDGFR-alpha/beta Downregulation Inhibits Tumorigenesis and Enhances TRAIL-Induced Apoptosis in Lung Cancer.* PLoS One, 2015. **10**(6): p. e0131729.
94. Shingyochi, Y., et al., *A Low-Level Carbon Dioxide Laser Promotes Fibroblast Proliferation and Migration through Activation of Akt, ERK, and JNK.* PLoS One, 2017. **12**(1): p. e0168937.
95. Alphonse, R.S., et al., *Activation of Akt protects alveoli from neonatal oxygen-induced lung injury.* Am J Respir Cell Mol Biol, 2011. **44**(2): p. 146-54.
96. LaRochelle, W.J., et al., *PDGF-D, a new protease-activated growth factor.* Nat Cell Biol, 2001. **3**(5): p. 517-21.

97. Alberts B, J.A., Lewis J, et al., *Signaling through Enzyme-Linked Cell-Surface Receptors*, in *Molecular Biology of the Cell*. 2002: New York: Garland Science.
98. Leary, S., et al., *Genetic Strain and Sex Differences in a Hyperoxia-Induced Mouse Model of Varying Severity of Bronchopulmonary Dysplasia.* Am J Pathol, 2019.
99. Syed, M., et al., *Hyperoxia causes miR-34a-mediated injury via angiopoietin-1 in neonatal lungs.* Nat Commun, 2017. **8**(1): p. 1173.
100. Zhuang, X.F., et al., *miR-34b inhibits the migration/invasion and promotes apoptosis of non-small-cell lung cancer cells by YAF2.* Eur Rev Med Pharmacol Sci, 2019. **23**(5): p. 2038-2046.
101. Zhou, Y.L., Y.J. Xu, and C.W. Qiao, *MiR-34c-3p suppresses the proliferation and invasion of non-small cell lung cancer (NSCLC) by inhibiting PAC1/MAPK pathway.* Int J Clin Exp Pathol, 2015. **8**(6): p. 6312-22.
102. Visser, Y.P., et al., *Apelin attenuates hyperoxic lung and heart injury in neonatal rats.* Am J Respir Crit Care Med, 2010. **182**(10): p. 1239-50.
103. Melgar-Lesmes, P., et al., *Apelin mediates the induction of profibrogenic genes in human hepatic stellate cells.* Endocrinology, 2010. **151**(11): p. 5306-14.
104. Ruiz-Camp, J., et al., *Targeting miR-34a/Pdgfra interactions partially corrects alveologenesis in experimental bronchopulmonary dysplasia.* EMBO Mol Med, 2019. **11**(3).
105. Oak, P., et al., *Attenuated PDGF signaling drives alveolar and microvascular defects in neonatal chronic lung disease.* EMBO Mol Med, 2017. **9**(11): p. 1504-1520.
106. Borghesi, A., et al., *Circulating endothelial progenitor cells in preterm infants with bronchopulmonary dysplasia.* Am J Respir Crit Care Med, 2009. **180**(6): p. 540-6.
107. Baker, C.D., et al., *Cord blood angiogenic progenitor cells are decreased in bronchopulmonary dysplasia.* Eur Respir J, 2012. **40**(6): p. 1516-22.
108. Hasan, J., et al., *Soluble vascular endothelial growth factor receptor 1 in tracheal aspirate fluid of preterm neonates at birth may be predictive of bronchopulmonary dysplasia/chronic lung disease.* Pediatrics, 2009. **123**(6): p. 1541-7.
109. Wang, K., et al., *A comparison of KL-6 and Clara cell protein as markers for predicting bronchopulmonary dysplasia in preterm infants.* Dis Markers, 2014. **2014**: p. 736536.
110. Tokuriki, S., et al., *Carboxyhemoglobin Formation in Preterm Infants Is Related to the Subsequent Development of Bronchopulmonary Dysplasia.* Dis Markers, 2015. **2015**: p. 620921.
111. Zegdi, R., et al., *Increased endogenous carbon monoxide production in severe sepsis.* Intensive Care Med, 2002. **28**(6): p. 793-6.
112. La Frano, M.R., et al., *Umbilical cord blood metabolomics reveal distinct signatures of dyslipidemia prior to bronchopulmonary dysplasia and pulmonary hypertension.* Am J Physiol Lung Cell Mol Physiol, 2018. **315**(5): p. L870-L881.

13 List of Publications

Jordi Ruiz-Camp, Jennifer Quantius, Ettore Lignelli, Philipp F Arndt, Francesco Palumbo, Claudio Nardiello, David E Surate Solaligue, Elpidoforos Sakkas, Ivana Mižíková, José Alberto Rodríguez-Castillo, István Vadász,William D Richardson, Katrin Ahlbrecht, Susanne Herold, Werner Seeger, Rory E Morty. *Targeting miR-34a/*Pdgfra *interactions partially corrects alveologenesis in experimental bronchopulmonary dysplasia.* EMBO Molecular Medicine 2019

14 Declaration of authorship

I declare that I have completed this dissertation single-handedly, without the unauthorized help of a second party and only with the assistance acknowledged therein. I have appropriately acknowledged and referenced all text passages that are derived literally from or are based on the content of published or unpublished work of others, and all information that relates to verbal communications. I have abided by the principles of good scientific conduct laid down in the charter of the Justus Liebig University of Giessen in carrying out the investigations described in the dissertation.

This paper was not previously presented to another examination board and has not been published.

_____ _____

City, Date Signature

15 Acknowledgements

First of all, I would like to thank my supervisor Dr. Rory Morty for giving me the opportunity to take my first steps into the world of science. Thank you for your vision, your encouragement and your constructive criticism. I always felt well guided under your tutelage.

Very special thanks go to Dr. Jordi Ruiz-Camp for sharing all your technical knowledge. Thank you for teaching me all the techniques I now know. I am grateful for your patience, honesty and support, you have been a true mentor to me.

Of course, I also would like to thank every other member from the laboratory for sharing your knowledge with me and for naturally accepting me into your ranks. Thank you for making the work load so light with all the jokes and fun we had. A special mention has to go to Lena, my partner in crime at the lab.

Many thanks also go to the charming technicians Diana and Nilifer for helping out where ever they could.

Last but not least, I thank my family, especially my parents, for giving me emotional support and strength when the times were tough. Thank you for always being there for me when needed. Without you I would have never gotten so far.